The Fascinating Turbulence and Magnetism of the Sun and stars

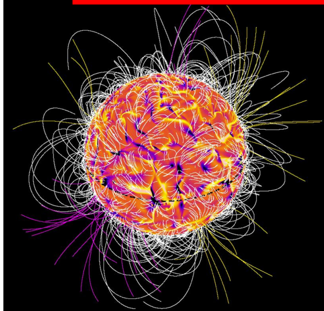

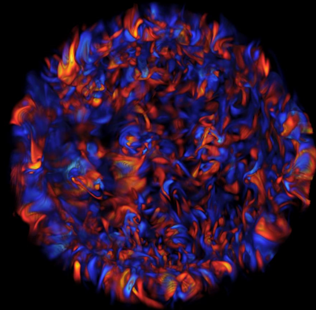

Allan Sacha Brun
Service d'Astrophysique/UMR AIM,
CEA/DSMDAPNIA/ Saclay
and J.Toomre, M.S. Miesch, M. Browning, B. Brown, L. Jouve,
A. Palacios, N. Featherstone, K. Auguston, N. Nelson

- Observational evidences of stellar magnetism
- 3D MHD simulations of the magnetic Sun
- 3D MHD simulations of other stellar spectral types

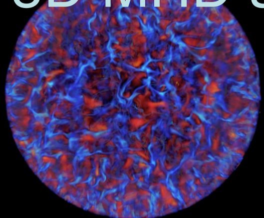

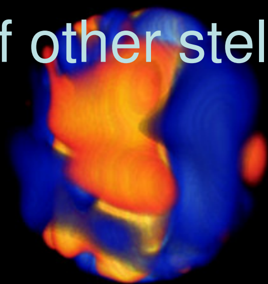

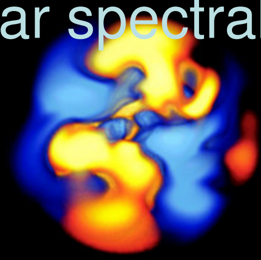

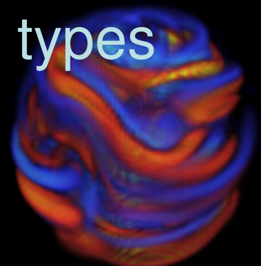

Magnetic Solar Cycle 23-24

(HAO, SST & Mt Wilson Data)

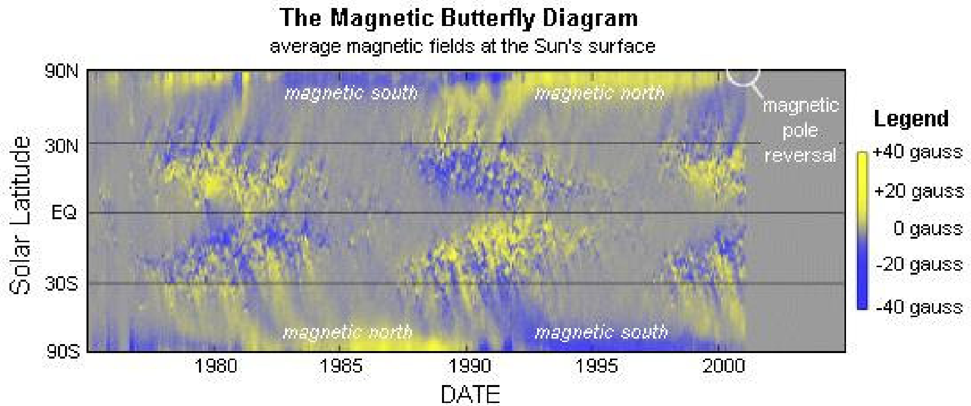

Regions

Quiet

Active

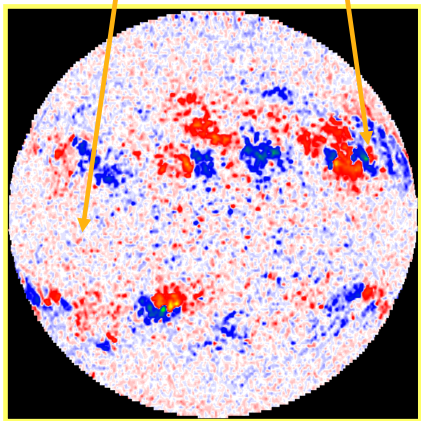

5895.9Å Na I

Magnétogramme

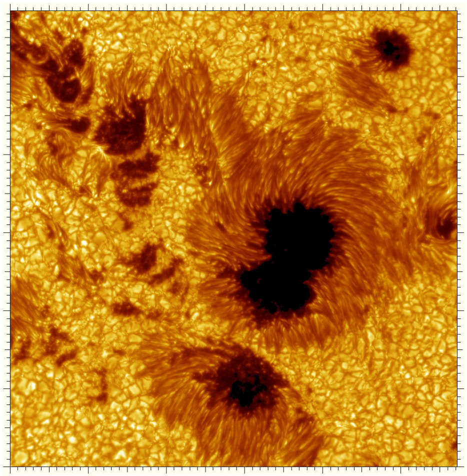

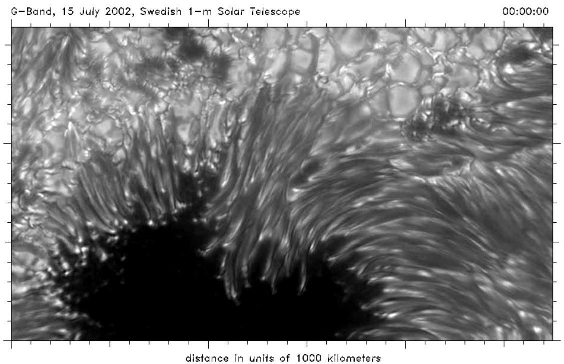

Small vs Large Scale Dynamos

Wide range of dynamical scales!

Solar Internal Rotation

Helioseismology Results

(GONG, MDI data)

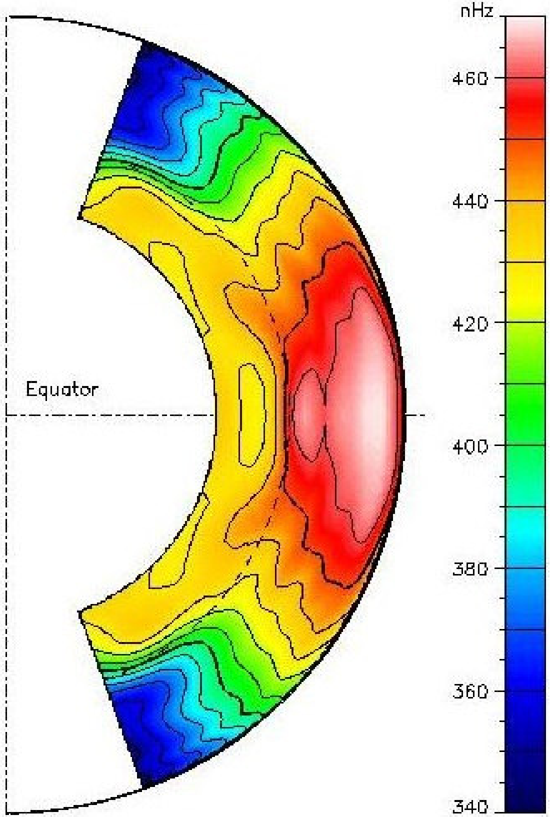

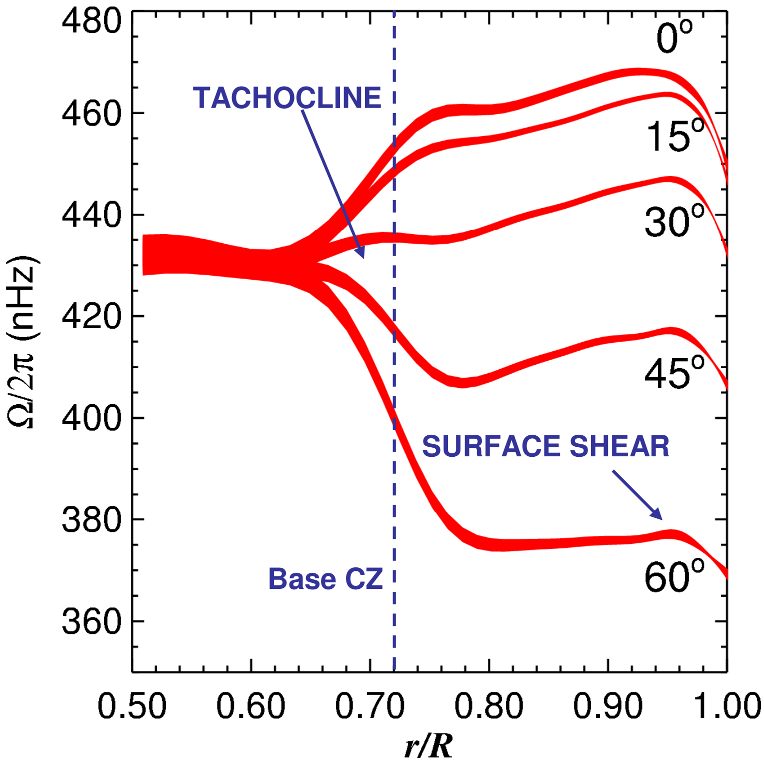

Modulation of Differential Rotation Amplitude with Cycle

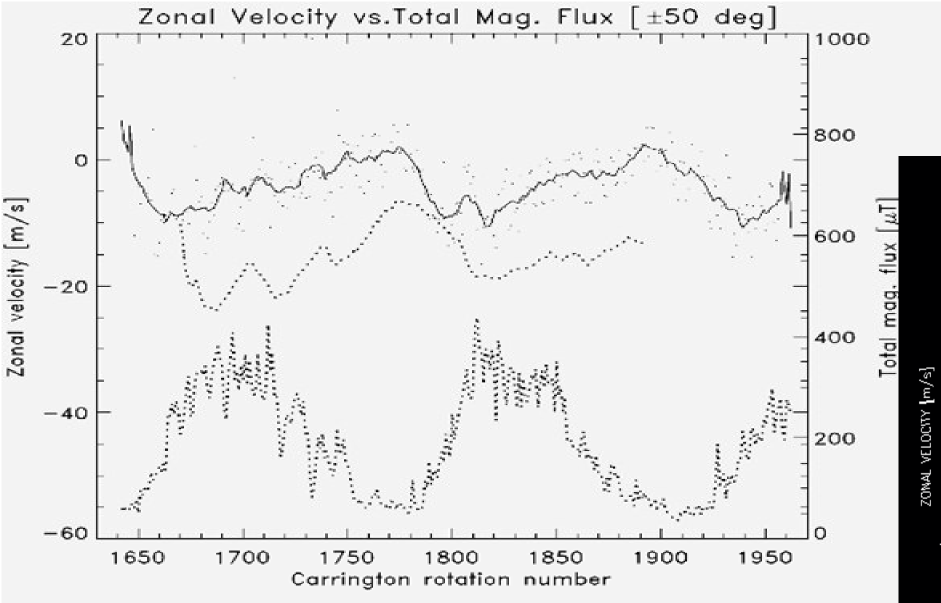

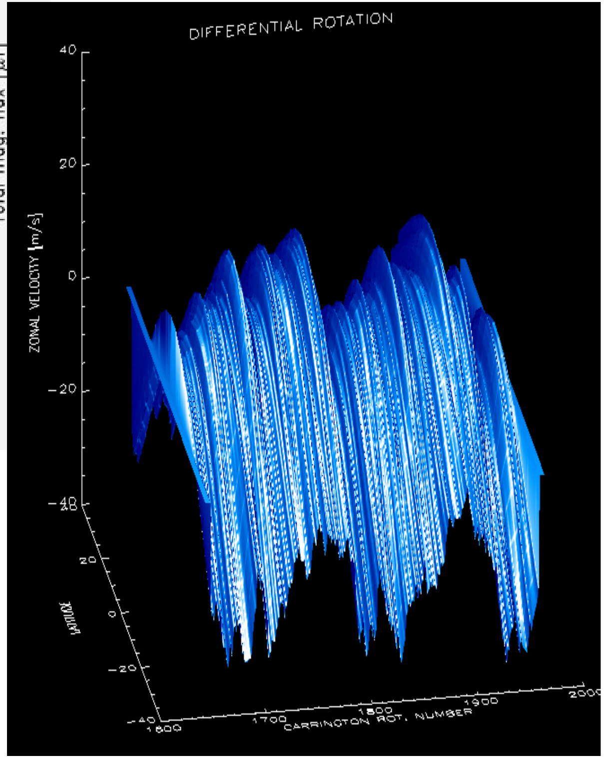

Courtesy of Ambroz

Meridional Circulation

More & more evidence for multi cellular MC

Mitra-Kaev & Thompson 2007

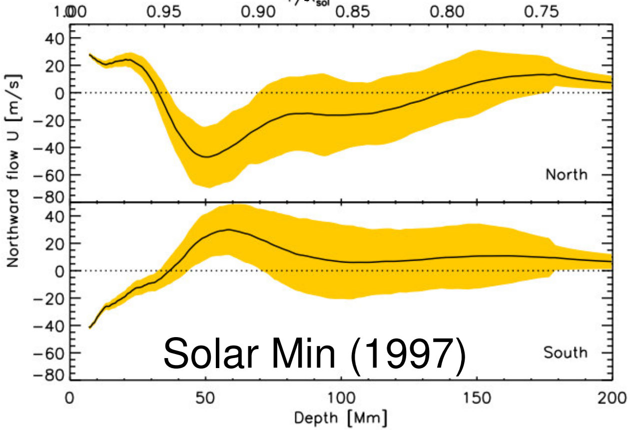

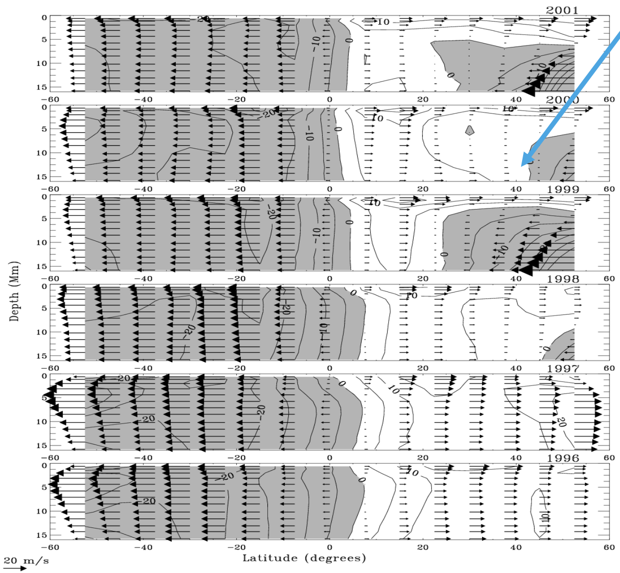

(Haber et al. 2002)

Influence of B (active region) on MC

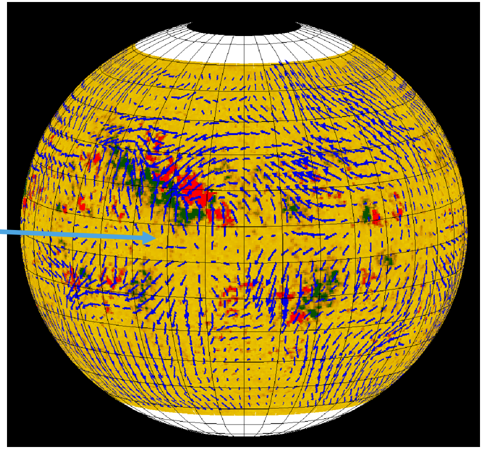

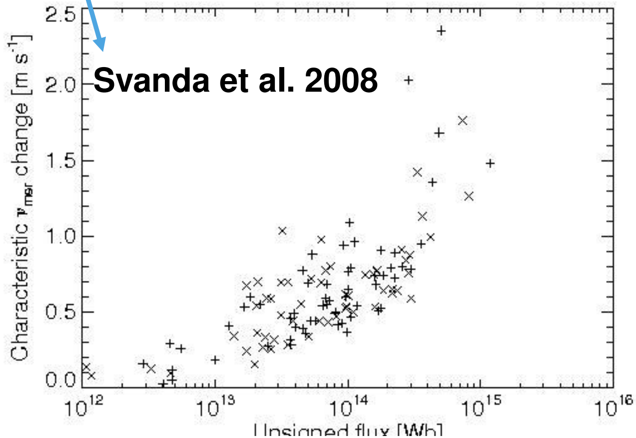

See also Hathaway et al. 1996, Gizon 2004, Zhao & Kosovichev 2004, etc…

Solar Cycle 22 (Yohkoh)

http://www.lmsal.com/SXT/homepage.html

Large variation in X (soft), small in visible

X light is a good proxy for stellar magnetism

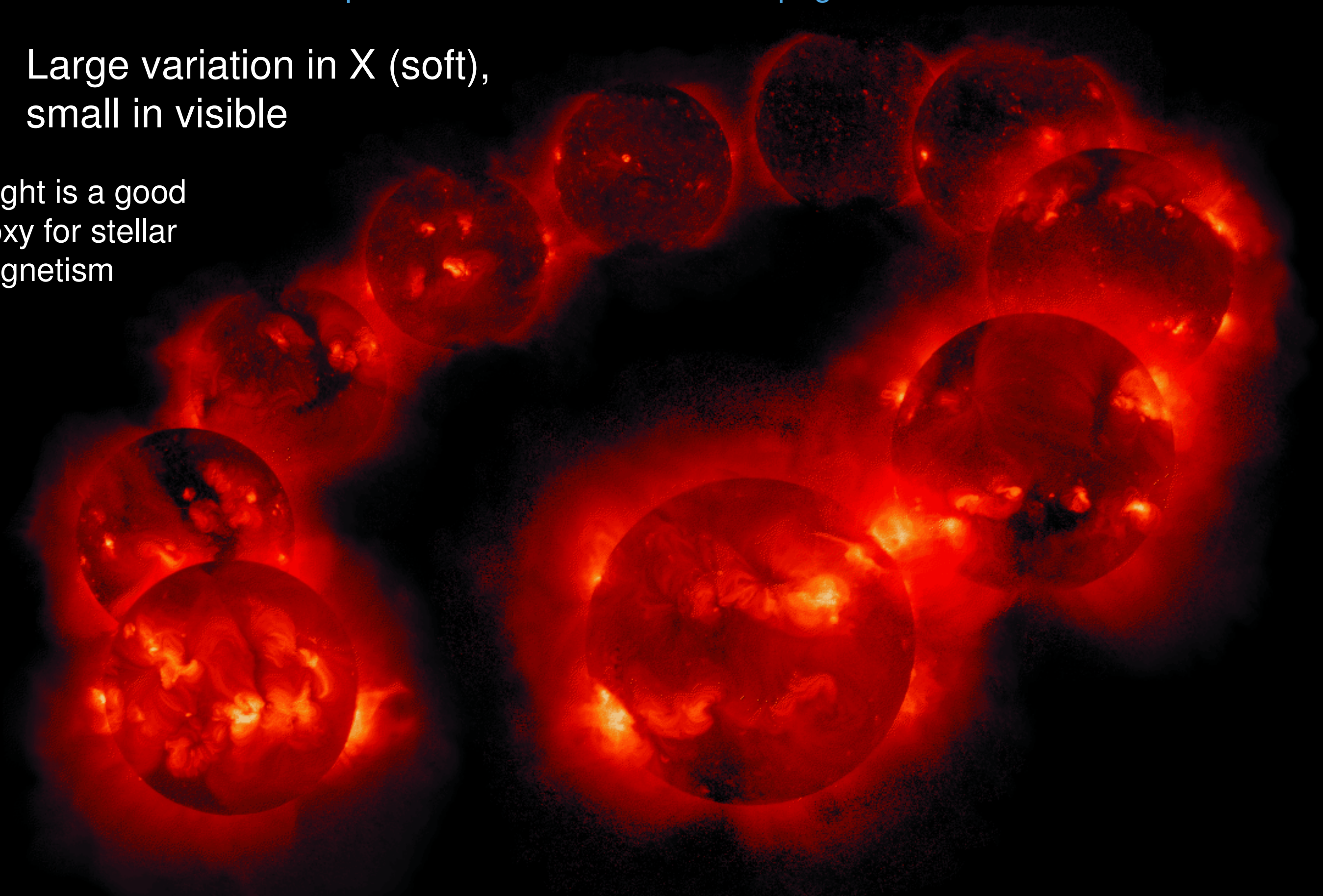

Stellar Magnetism: X Luminosity
(ROSAT All Sky Survey, EspaDONS)

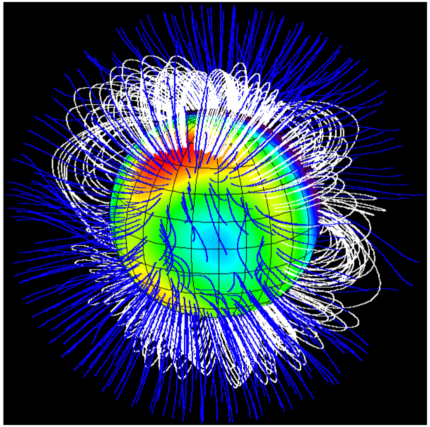

Observations Narval
(J.F. Donati,
massive star tau Scorpii)

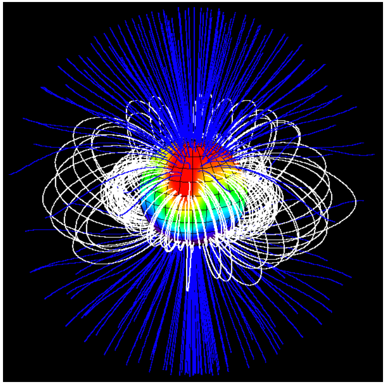

ultra-cool star V374 Pegasi

Good correlation between activity level and surface convection

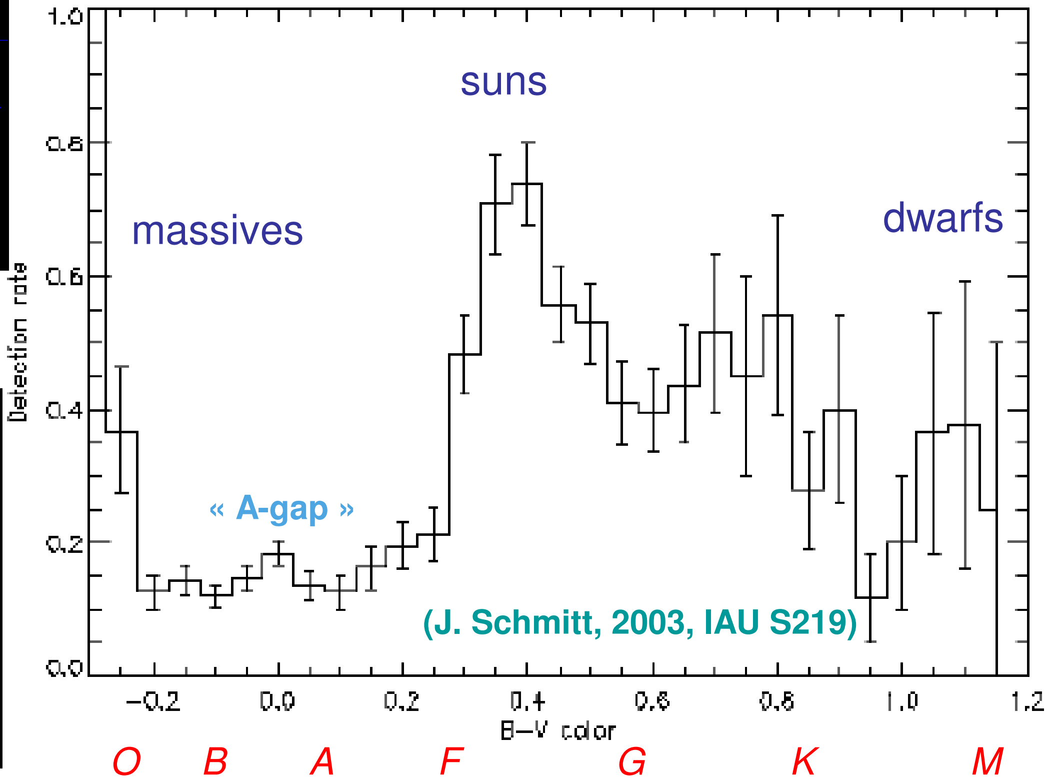

Co,nvection in Stellar Interior

Transition between envelope and core convection: M ~1.3 Msol

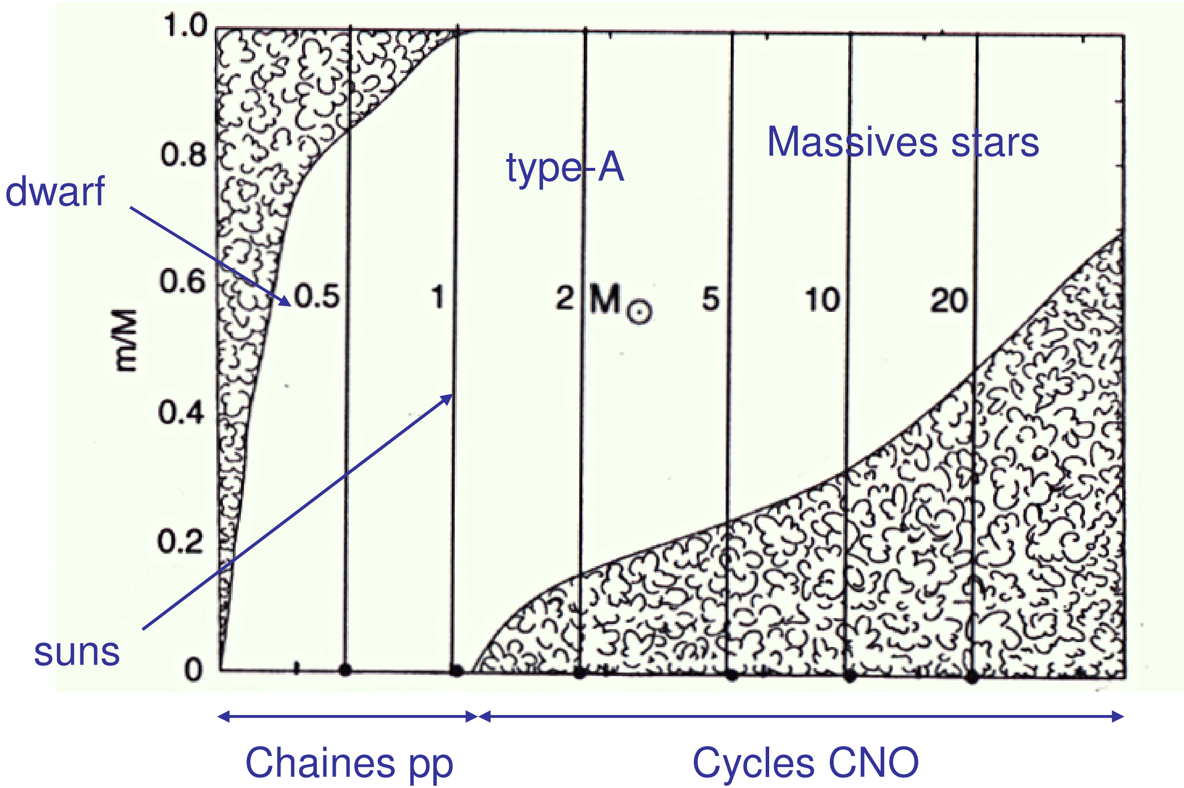

Solar Type Stars (late F, G and early K-type)

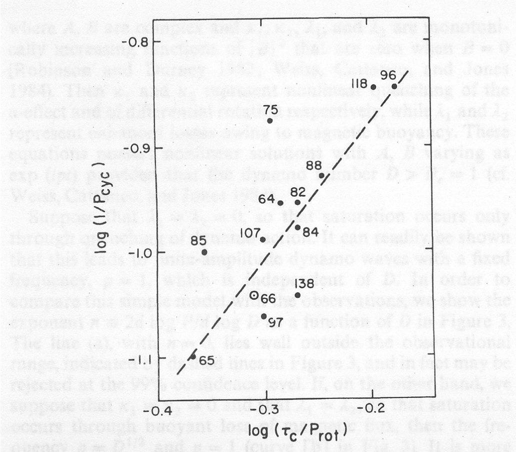

FIG. 2.—Log $(1/P_{cyc})$ vs. log (τ_c/P_{rot}) for the stars of Table 1. The dashed line is a linear least squares fit to the data.

In stars activity depends on rotation & convective overturning time via Rossby nb $Ro=P_{rot}/\tau$

$\langle R'_{HK}\rangle = Ro^{-1}$

<u>Over 111 stars in HK project (F2-M2):</u>

31 flat or linear signal

29 irregular variables

51 + Sun possess magnetic cycle

Wilson 1978

Baliunas et al. 1995

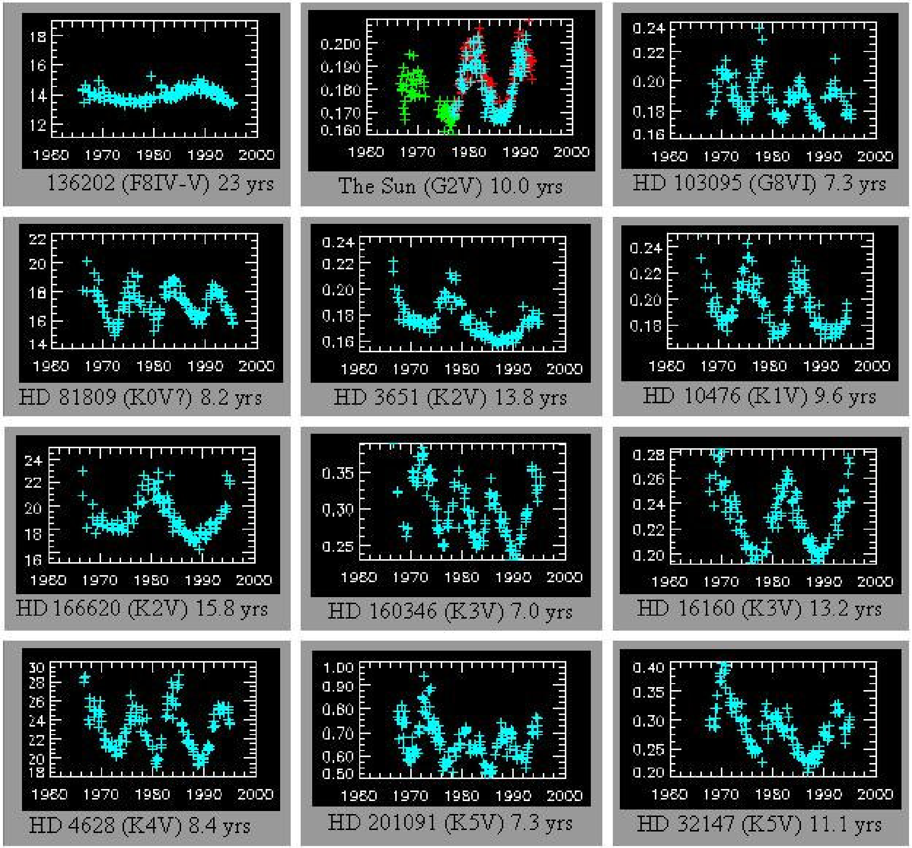

CaII H & K lines , $\langle R'_{HK}\rangle$

F to K stars (continued)

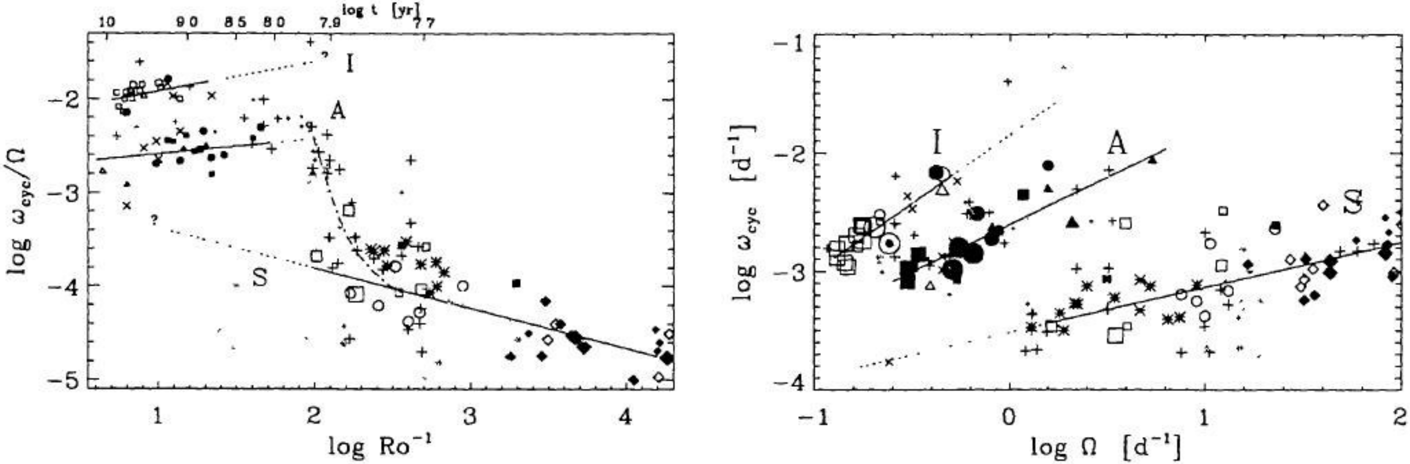

Figure 3. Left panel: same as Fig. 2 left, but including cycles based on P_{rot} variation in RS CVns (new +), CV secondaries (open ◇), Algols (∗), and contact binaries (gray ◇). Right panel: same as Fig. 2 right, but including the additional P_{cyc} in the left panel.

Single power law can fit data: ω_cycle ~ $\Omega^{-0.09}$, but with much higher dispersion in fit

Saar & Brandenburg, 99; Saar 02, 05

Solar Analogs

Name	T_{eff} K	log(g) [cm.s^{-2}]	[M/H] [Sun]	Mass $M_\odot$	Age Gyr	$v \sin i$ km s^{-1}	$\mathbf{P^{eq}_{rot}}$ **(d)**	$d\Omega$ (rad.d^{-1})	inclination (°)
Sun	5770	4.44	0.00	1.0	4.3 ± 1.7	1.7	**24**	0.05	–
HD 146233	5791 ± 50	4.41 ± 0.06	0.03 ± 0.03	0.98 ± 0.13	$4.7^{+2.7}_{-2.7}$	2.1 ± 0.5	$\mathbf{22.7 \pm 0.5}$	–	70^{+20}_{-25}
HD 76151	5790 ± 50	4.55 ± 0.06	0.07 ± 0.03	1.24 ± 0.12	$3.6^{+1.8}_{-2.3}$	1.2 ± 0.5	$\mathbf{20.5 \pm 0.3}$	–	30 ± 15
HD 73350	5802 ± 50	4.48 ± 0.06	0.04 ± 0.03	1.01 ± 0.14	$4.1^{+2.0}_{-2.7}$	4.0 ± 0.5	$\mathbf{12.3 \pm 0.1}$	0.2 ± 0.2	75^{+15}_{-20}
HD 190771	5834 ± 50	4.44 ± 0.06	0.14 ± 0.03	0.96 ± 0.13	$2.7^{+1.9}_{-2.0}$	4.3 ± 0.5	$\mathbf{8.8 \pm 0.1}$	0.12 ± 0.03	50 ± 10

Table 3. Magnetic quantities derived from the set of magnetic maps. We list the mean unsigned magnetic field ($B_{\rm mean}$), the fraction of the large-scale magnetic energy reconstructed in the poloidal field component and the fraction of the *poloidal* magnetic energy in the dipolar ($\ell = 1$), quadrupolar ($\ell = 2$) and octopolar ($\ell = 3$) components. In the last column, we also list $\log R'_{\rm HK}$ values derived from our sets of Stokes I spectra.

Name	$B_{\rm mean}$ (G)	pol. en. (% tot)	dipole (% pol)	quad. (% pol)	oct. (% pol)	$\log R'_{\rm HK}$
HD 146233	3.6 ± 1	99.3 ± 0.2	34 ± 6	56 ± 6	10 ± 10	-4.85 ± 0.02
HD 76151	5.6 ± 2	93 ± 6	79 ± 13	18 ± 8	3 ± 3	-4.69 ± 0.02
HD 73350	42 ± 7	52 ± 3	24 ± 5	29 ± 8	33 ± 5	-4.48 ± 0.02
HD 190771	51 ± 6	34 ± 1	43 ± 8	20 ± 2	23 ± 4	-4.42 ± 0.02

Petit et al. 2008, MNRAS

ESPADON/NARVAL

Solar Analogs

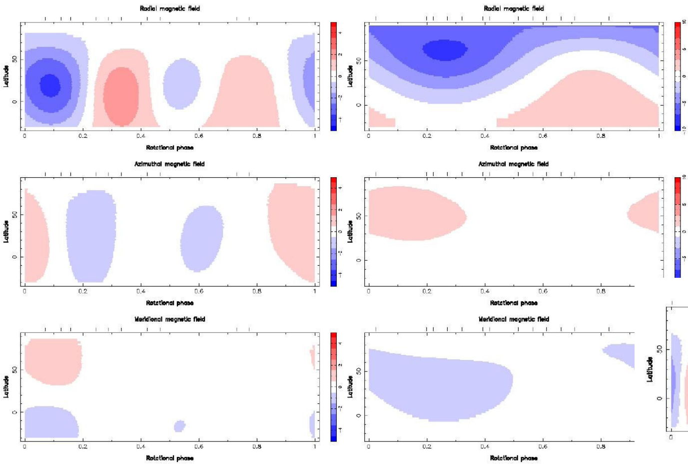

Figure 4. Magnetic maps of HD 146233 and HD 76151 (left and right panel, respectively). Each chart illustrates the
onto one axis of the spherical coordinate frame. The magnetic field strength is expressed in Gauss. Vertical ticks above the
the observed rotational phases. Note that color scales are not the same for every star.

Faster the solar analogs rotate more toroidal
Field contribution they possess.

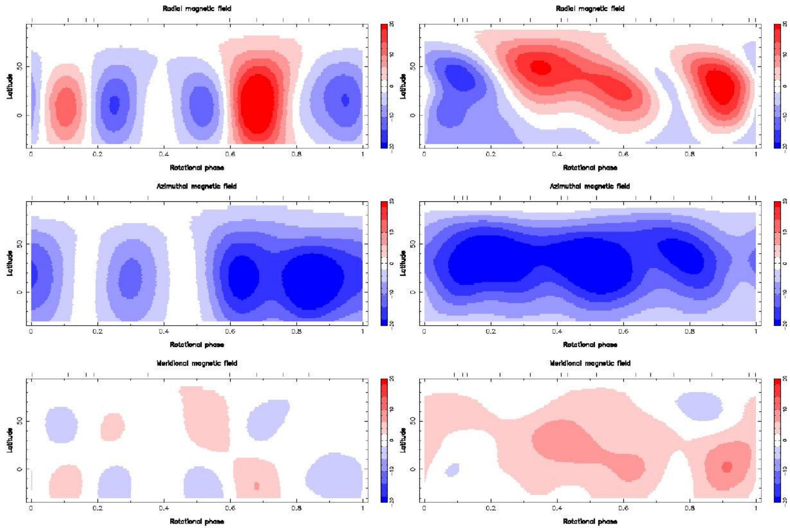

Figure 5. Same as Fig. 4, for HD 73350 (left panel) and HD 190771 (right panel).

Petit et al. 2008, MNRAS

ESPADON/NARVAL

Modelling Stars

- 1-D secular approach

  1. Standard microscopic models + Mixing Length Treatment
  2. Models with macroscopic processes (rotation, secular MHD)

- 2-D mean field

  1. Kinematic Mean field dynamo (α-ω or Babcock-Leigthon FT)
  2. Nonlinear mean field models (Λ effect, Malkus-Proctor feedback)

- 3-D MHD

  1. Local box simulations (high res/turbulent but lack global effect)
  2. Stars in the box approach (no center pb but outer BC's/interpol special)
  3. Stars in sphere or spherical shells (correct topology, mean flows less turbulent states)

Convective Motions (radial velocity Vr)

(Brun & Toomre 2002, ApJ, 570, 865)

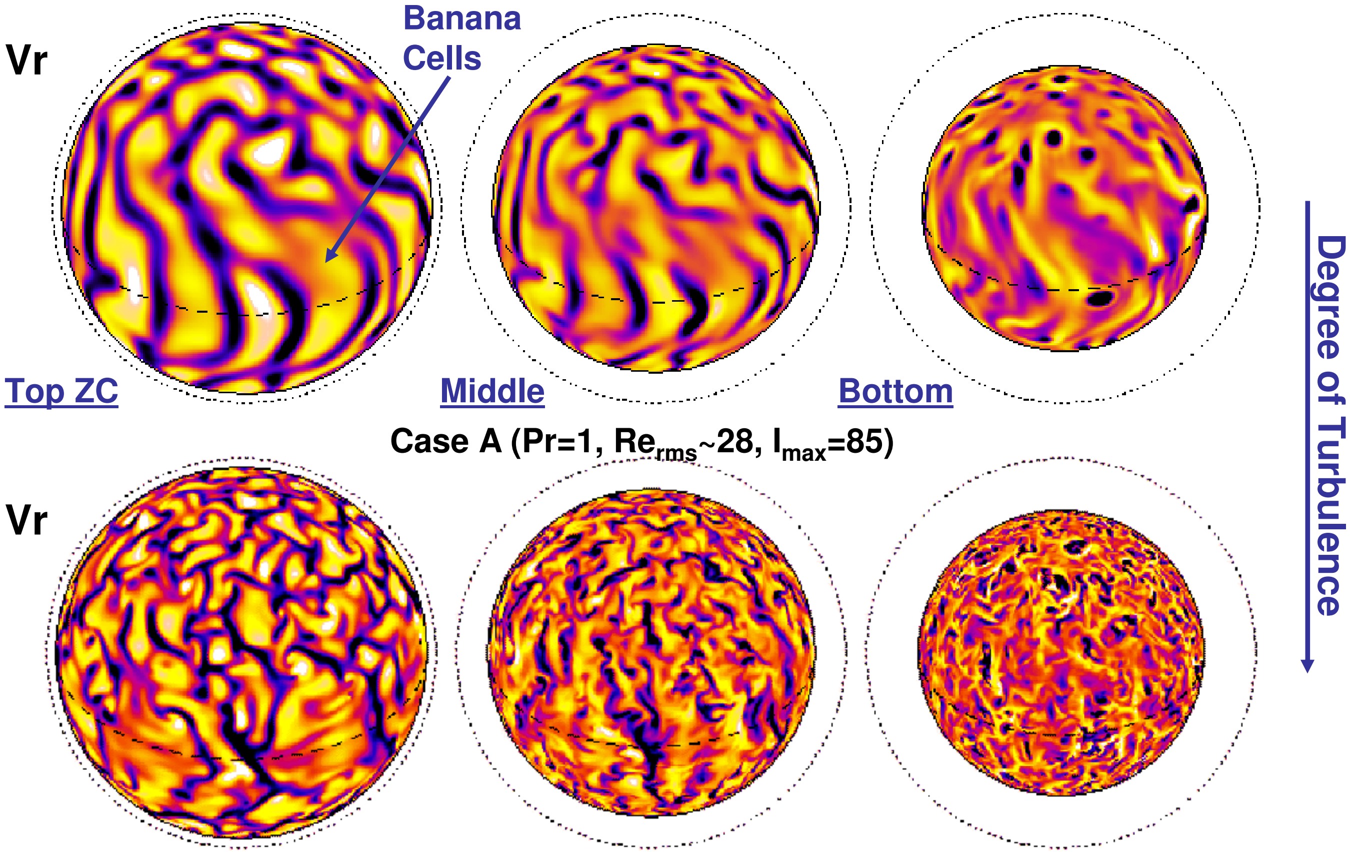

Case A (Pr=1, Re_{rms}~28, l_{max}=85)

Case D (Pr=0.25, Re_{rms}~410, l_{max}=340)

Mean Angular Velocity Ω

(Brun & Toomre 2002, ApJ 570, 865)

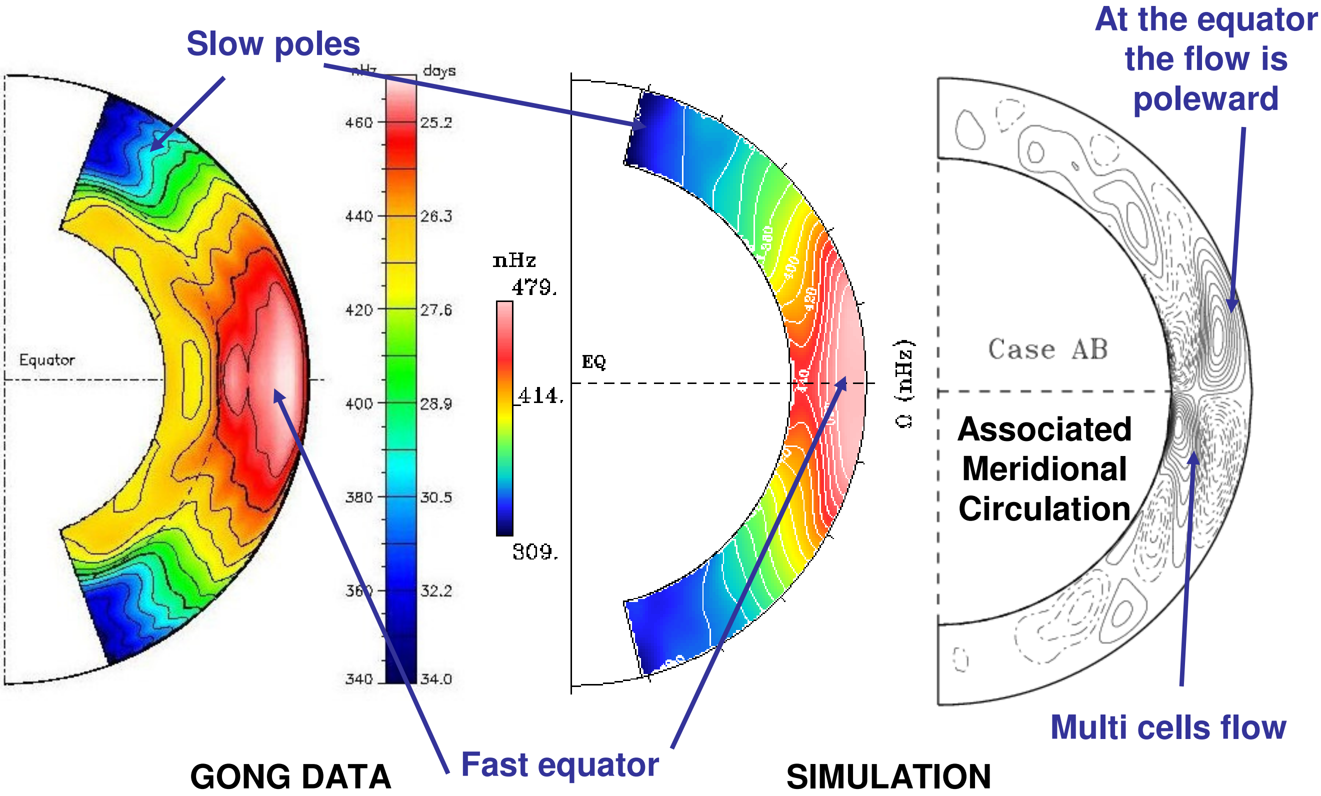

Angular Momentum Flux (MHD case)

Because of our choice of stress free and match to a Potential field boundary conditions, the total angular mometum L is conserved. Its transport can be expressed as the sum of 5 fluxes:

F_tot = F_Hydro + F_Maxwell + F_MeanB

with F_Hydro= F_viscous + F_Reynolds + F_meridional_circulation

In spherical coordinates:

F_r and F_θ are the radial and latitudinal angular momentum fluxes:

$$F_r = \hat{\rho} r \sin\theta \left[-\nu r \frac{\partial}{\partial r}\left(\frac{\hat{v}_\varphi}{r}\right) + \widehat{v'_r v'_\varphi} + \hat{v}_r (\hat{v}_\varphi + \Omega_0 r \sin\theta) - \frac{1}{4\pi\hat{\rho}} (\widehat{B'_r B'_\varphi} + \hat{B}_r \hat{B}_\varphi) \right]$$

$$F_\theta = \hat{\rho} r \sin\theta \left[-\nu \frac{\sin\theta}{r} \frac{\partial}{\partial \theta}\left(\frac{\hat{v}_\varphi}{\sin\theta}\right) + \widehat{v'_\theta v'_\varphi} + \hat{v}_\theta (\hat{v}_\varphi + \Omega_0 r \sin\theta) - \frac{1}{4\pi\hat{\rho}} (\widehat{B'_r B'_\varphi} + \hat{B}_r \hat{B}_\varphi) \right]$$

Transport of ang. mom. by diffusion, advection, merid. circ., Maxwell stresses & Mean B

Angular Momentum Balance

(Brun & Toomre 2002, ApJ, 570, 865)

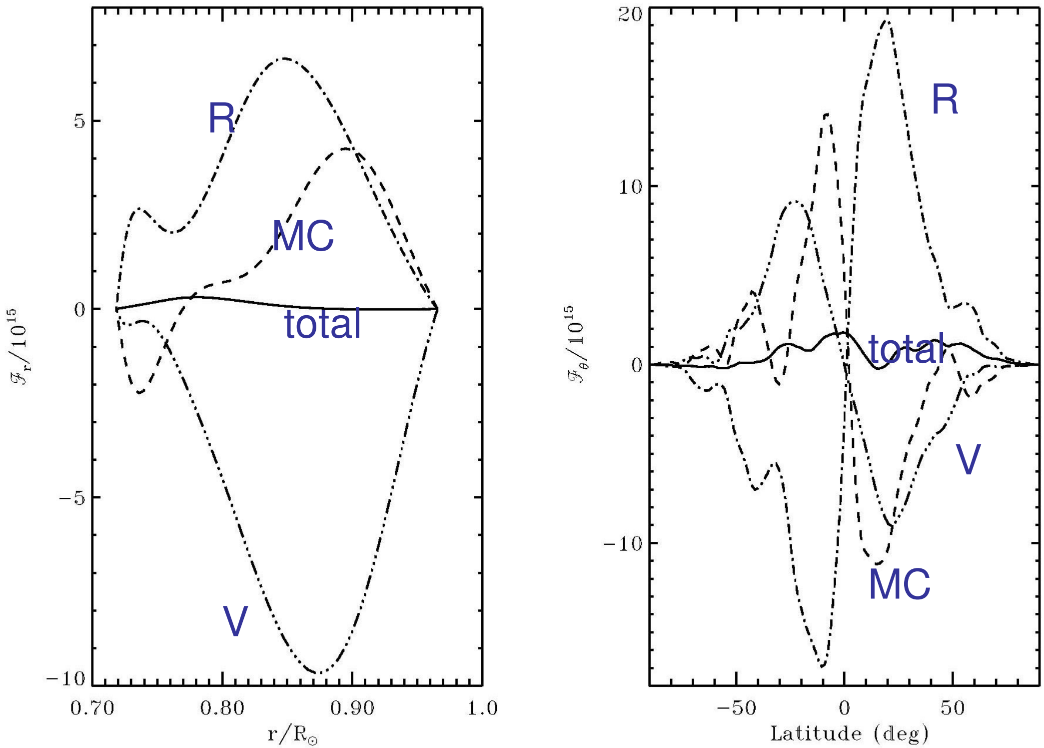

The transport of angular momentum by the Reynolds stresses is directed toward the equator (opposite to meridional circulation) and is at the origin of the equatorial acceleration

Taylor-Proudman Theorem & Thermal Wind

The curl of the momentum equation gives the equation for vorticity $\omega = \vec{\nabla} \times \vec{v}$ **:**

$$\frac{\partial \vec{\omega}}{\partial t} + \vec{v}.\vec{\nabla}\vec{\omega} - \vec{\omega}.\vec{\nabla}\vec{v} = \nu \vec{\nabla}^2 \vec{\omega} + \frac{1}{\rho^2} \vec{\nabla}\rho \wedge \vec{\nabla} p \qquad \text{(a)}$$

Taylor-Proudman Theorem:

In a stationary state, the φ component of (a) can be simplified to:

$$2\Omega \frac{\partial \hat{v}_\varphi}{\partial z} = 0$$ **=> vφ is cst along z**

the differential rotation is cylindrical (Taylor columns) and the flows quasi 2-D.

Thermal Wind:

The presence of cross gradient between p and ρ (baroclinic effects) can break this constraint (as well as Reynolds & viscous stresses and magnetic field) :

$$2\Omega \frac{\partial \hat{v}_\varphi}{\partial z} = -\frac{1}{\hat{\rho}^2} \vec{\nabla}\hat{\rho} \wedge \vec{\nabla}\hat{p}\Big|_\varphi = \frac{1}{\hat{\rho} C_p} \left[\vec{\nabla}\hat{S} \wedge -\hat{\rho}\vec{g}\right]\Big|_\varphi = \frac{g}{r C_p} \frac{\partial \hat{S}}{\partial \theta}$$

Baroclinicity

(Brun & Toomre 2002, ApJ, 570, 865)

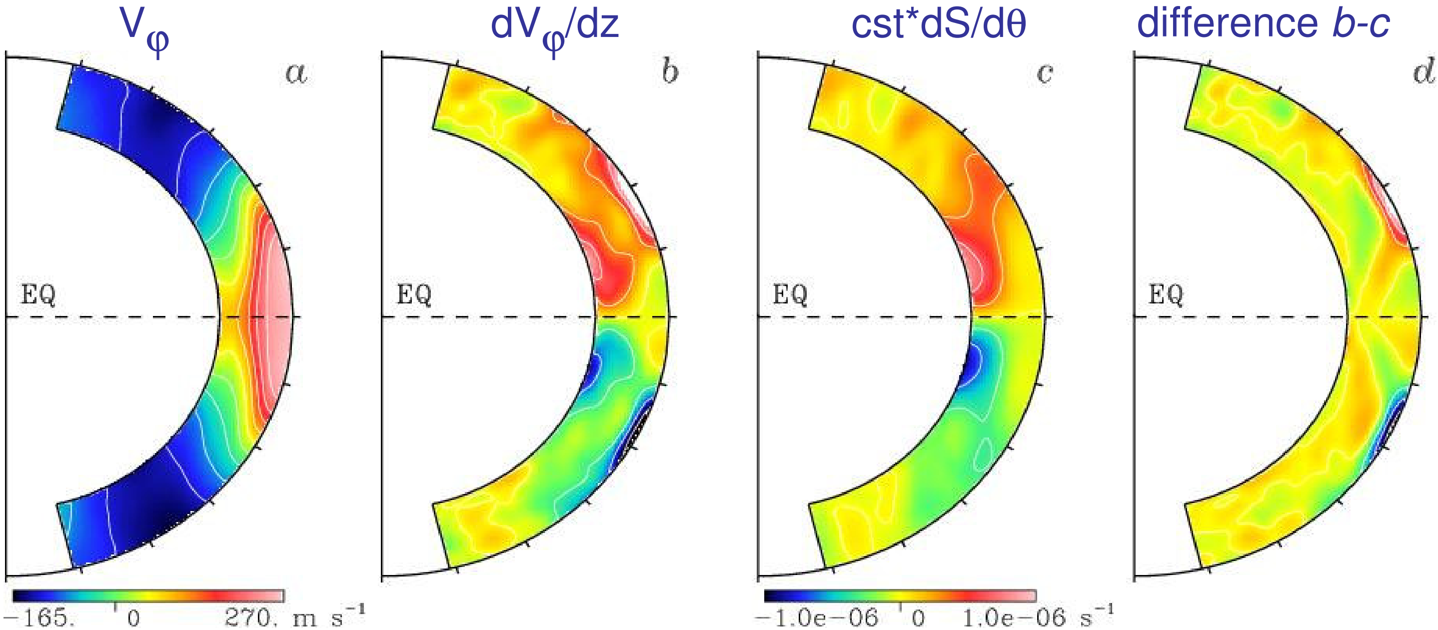

The thermal wind contributes for some but not all of the non cylindrical differential rotation achieved in our simulation.
Reynolds stresses are the dominant players confirming the dynamical origin of Ω

Latitudinal Heat Flux Balance

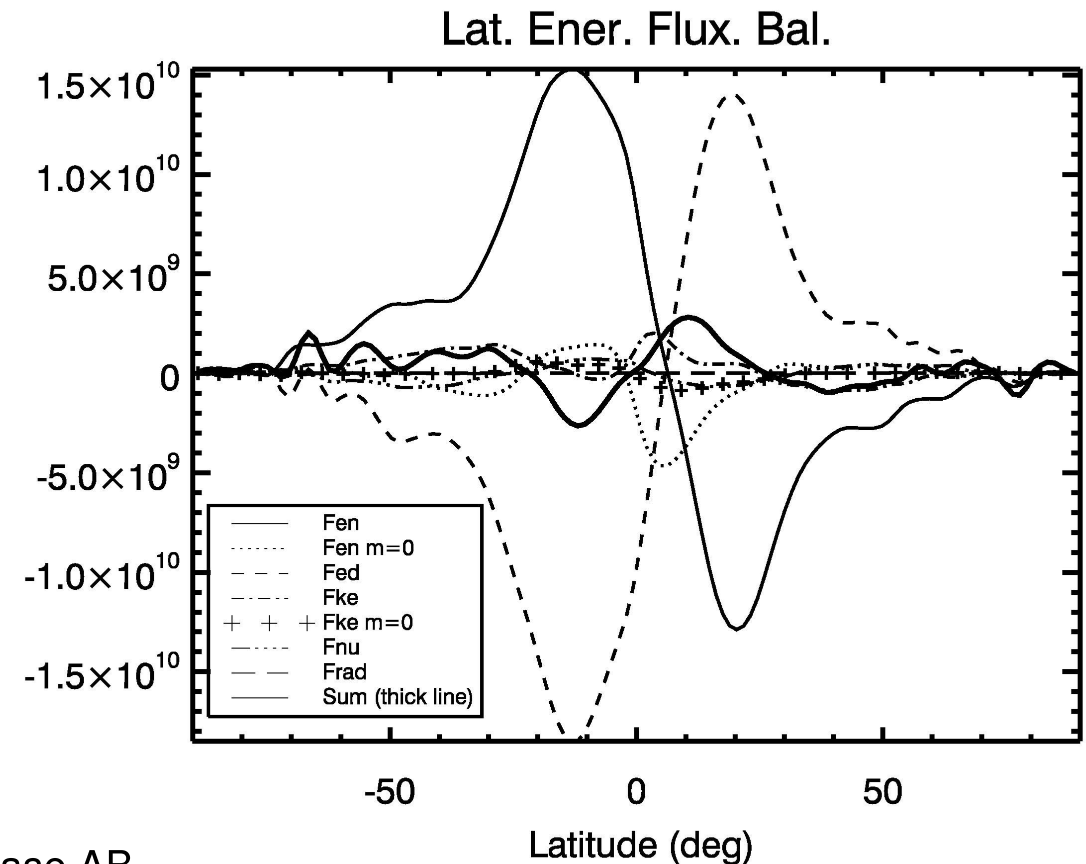

Laminar case AB
Brun & Toomre ApJ 2002

Thermal BC's Influence on Ω

No imposed S_{bot}

$$S(r_{bot}, \theta) = a_2\, Y_2^0 + a_4\, Y_4^0$$

Best Case

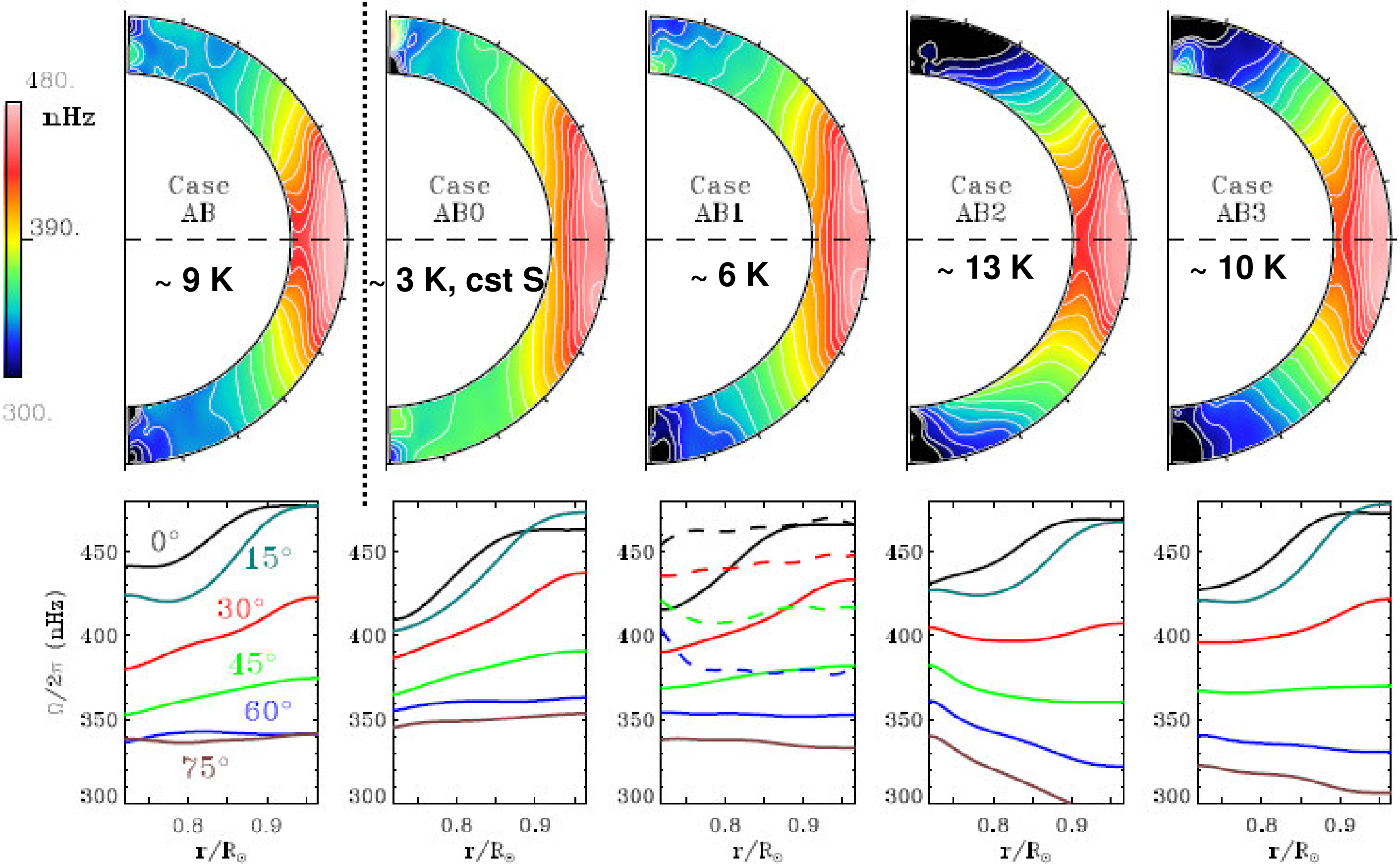

Miesch, Brun & Toomre 2006 ApJ, 641, 618 ; see also Rempel 2005

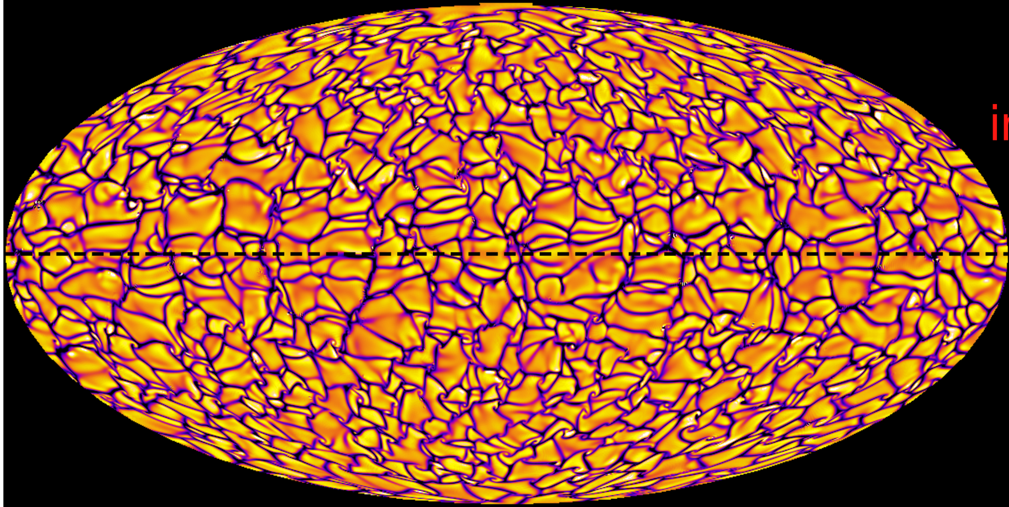

Vr and Temperature
in high resolution solar
convection

Density contrast
quite important
to get small scales

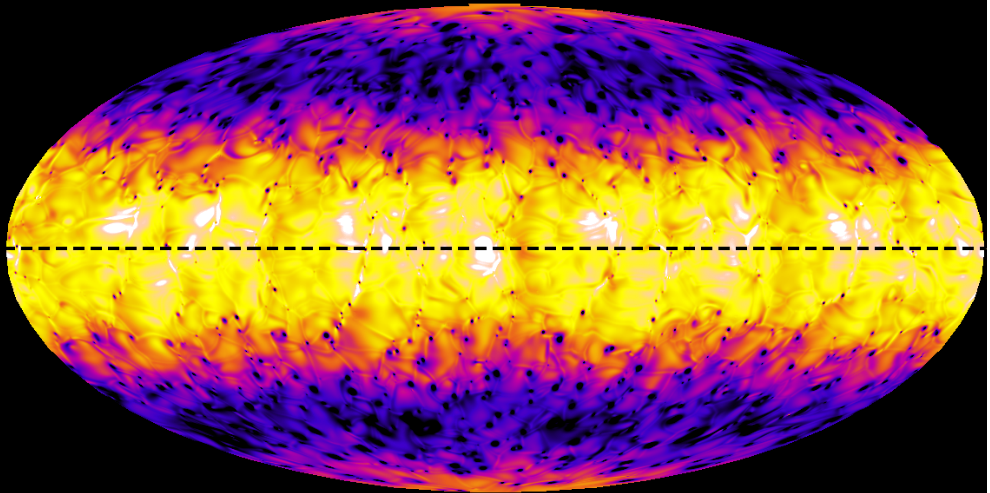

Resolution ~1500^3

Miesch, Brun, Derosa,
Toomre, 2008 ApJ, 673, 557

Convective Motions (v_r)

Resolution~ 1500^3
Re=VrmsD/ν~1000
Pr=0.25

depth=0.96 R

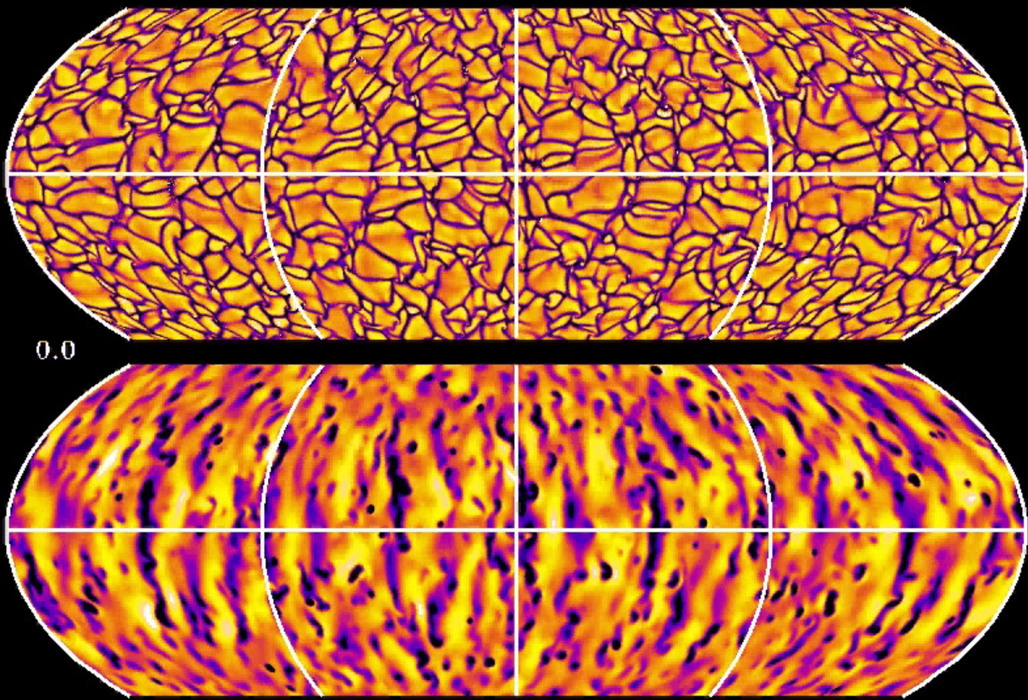

(Brun & Toomre,
2002, ApJ, 570, 865
Miesch, Brun, Derosa & Toomre, 2008, ApJ)

Meridional Circulation & Differential Rotation

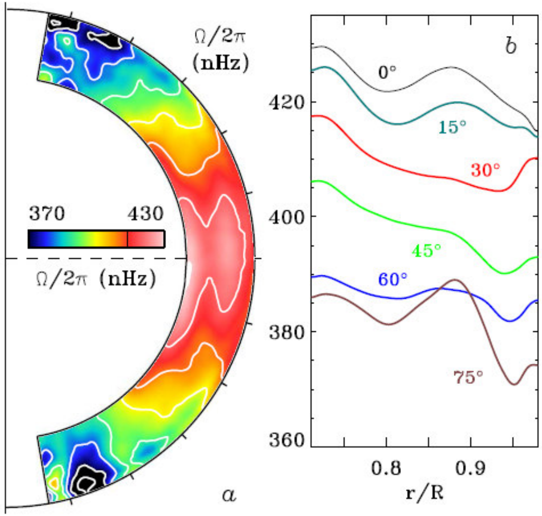

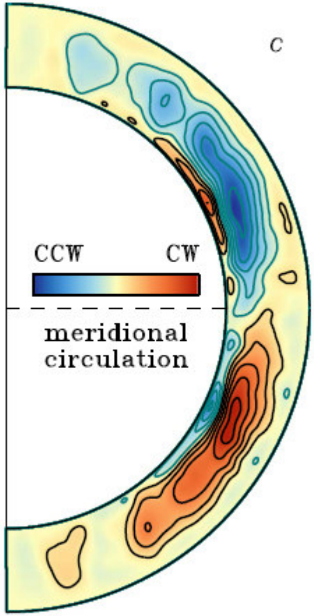

Large fluctuations, average out over long (> month) time avg

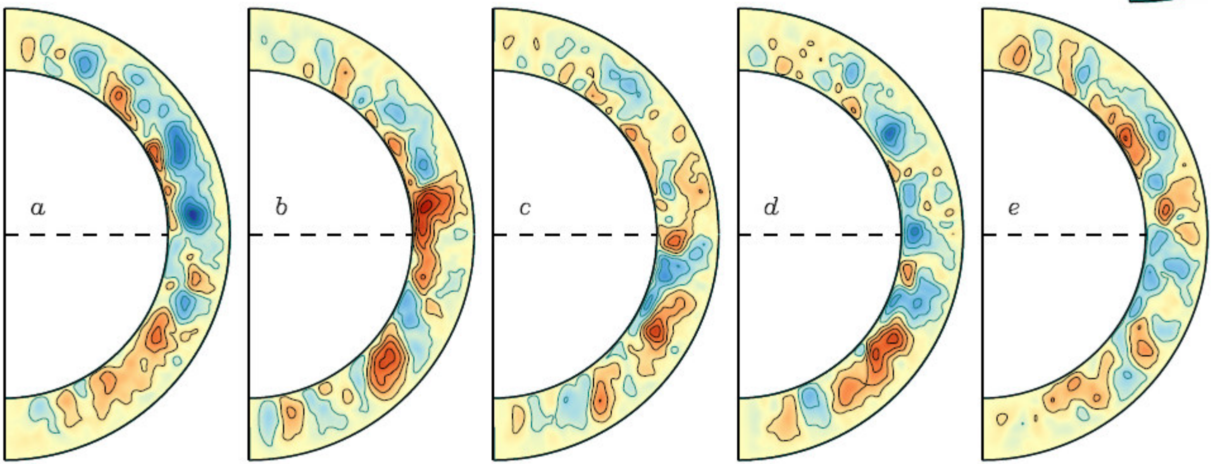

Case F

2D Mean Field models: Babcock-Leighton

Standard model: 1 cell per hemisphere

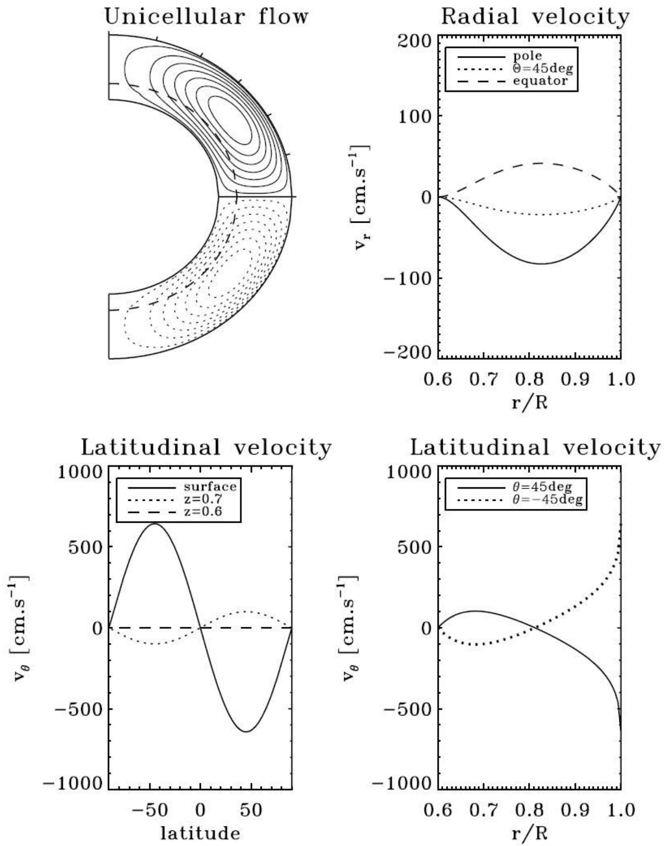

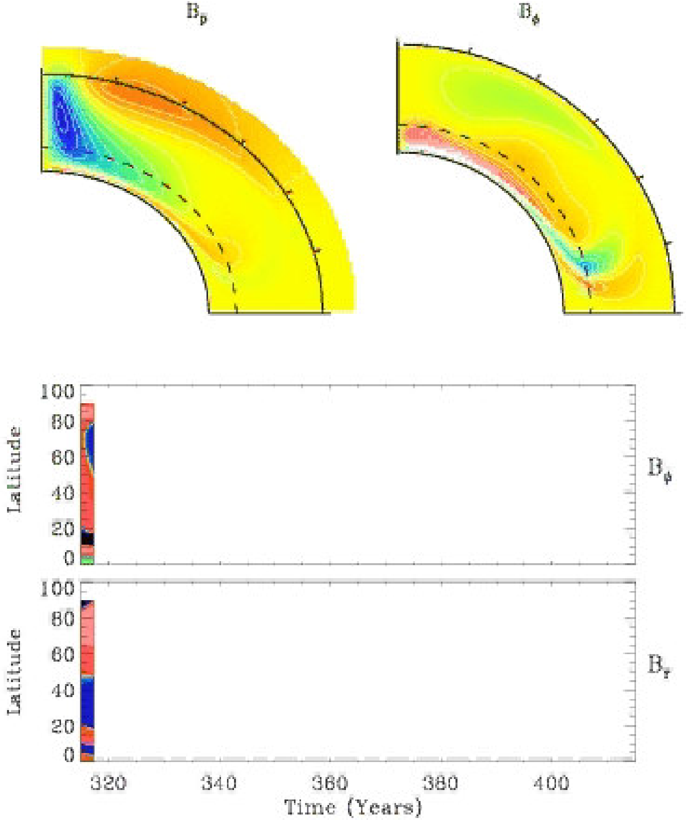

Jouve & Brun, 2007 A&A, 474, 239

Check Benchmark international: Jouve et al. 2008, A&A

2D Mean Field models: Babcock-Leighton

2 cells in latitude, 2 in radius per hemisphere

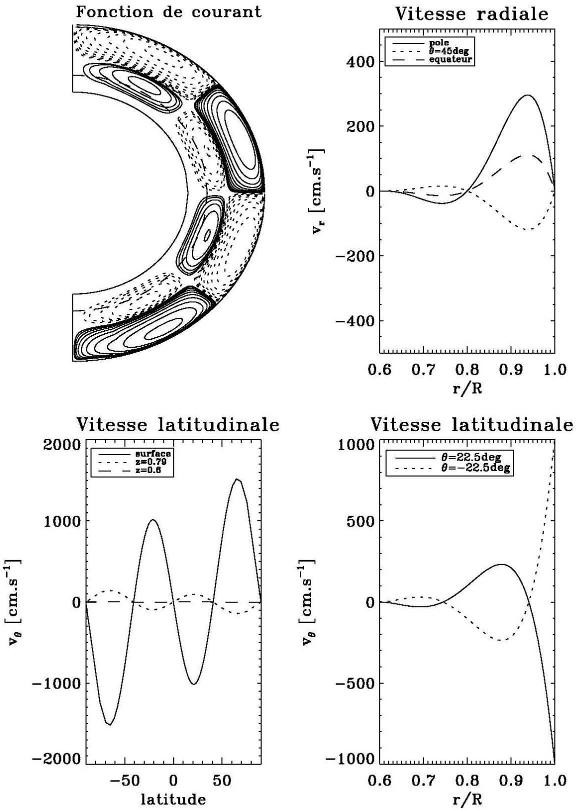

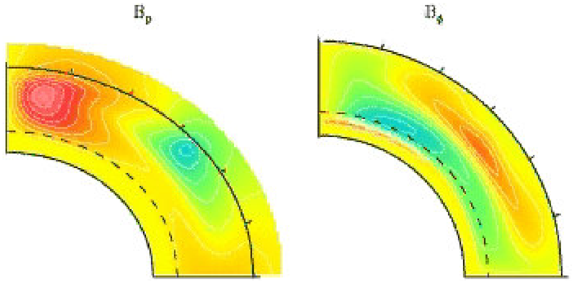

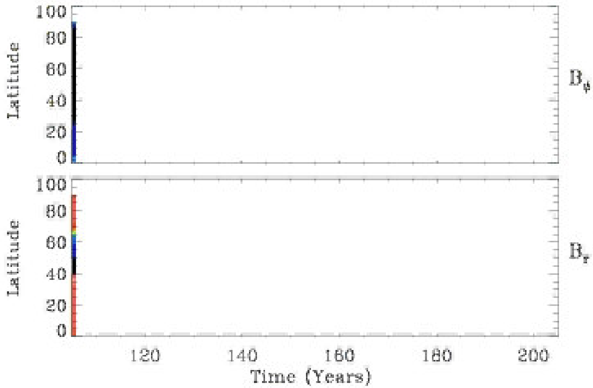

Slow down cycle period:
$T \sim v_0^{-0.35} \eta_t^{-0.4} s_0^{0.05}$

For parameter values identical to 1 cell case, find T=45 yr instead of 22, possible to get 22

Jouve & Brun, 2007 A&A, 474, 239

Magnetic Convection

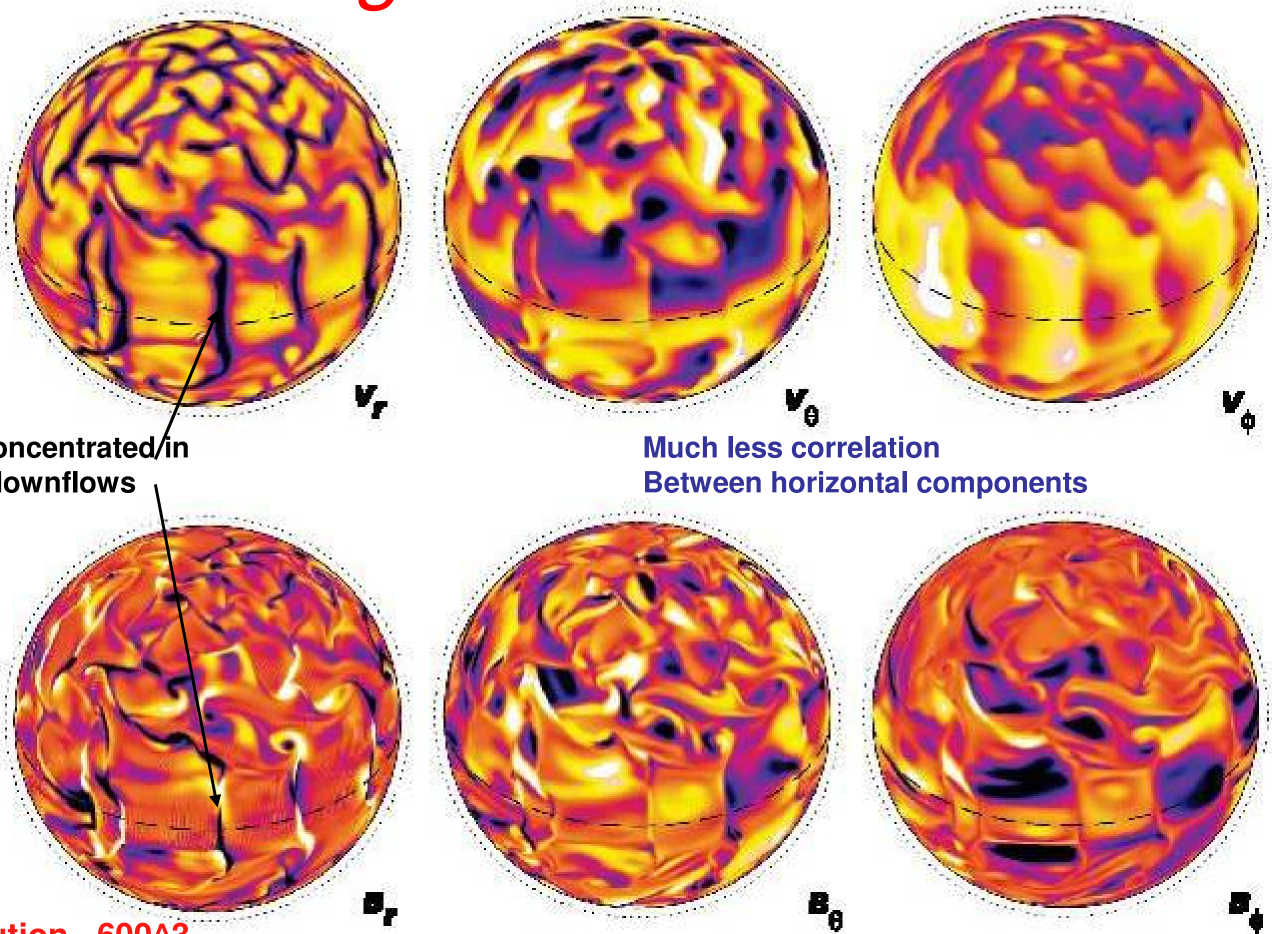

Br concentrated in the downflows

Much less correlation Between horizontal components

Resolution~ 600^3
Re=VrmsD/ν~150,P=0.25, Pm=4

MAGNETIC CASE M3 (Brun, Miesch, Toomre 2004)

Toroidal Field in Convection

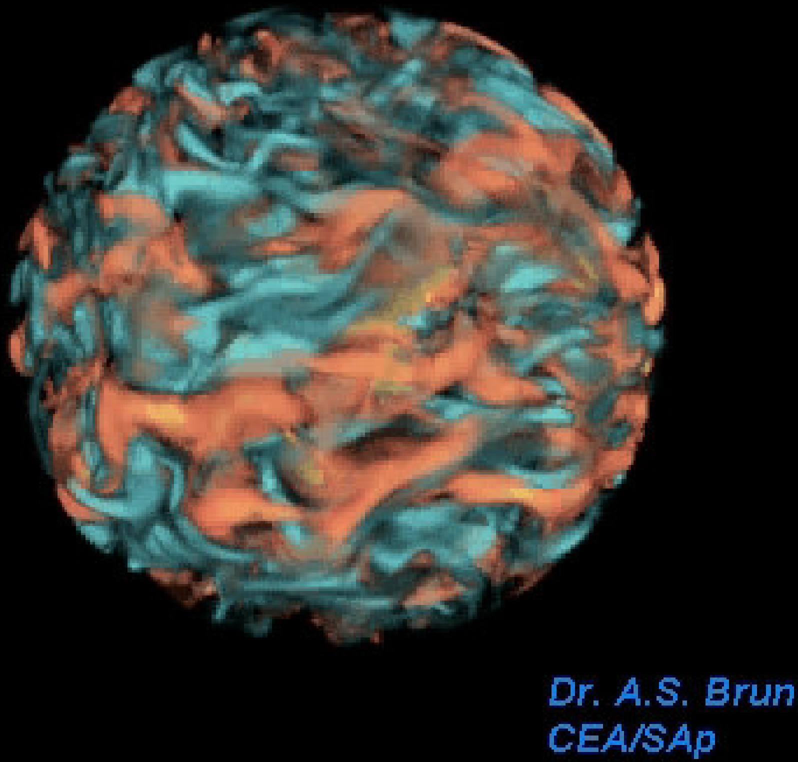

longitudinal component of B (Pm=4)

Dynamo Effect –Magnetic Energy

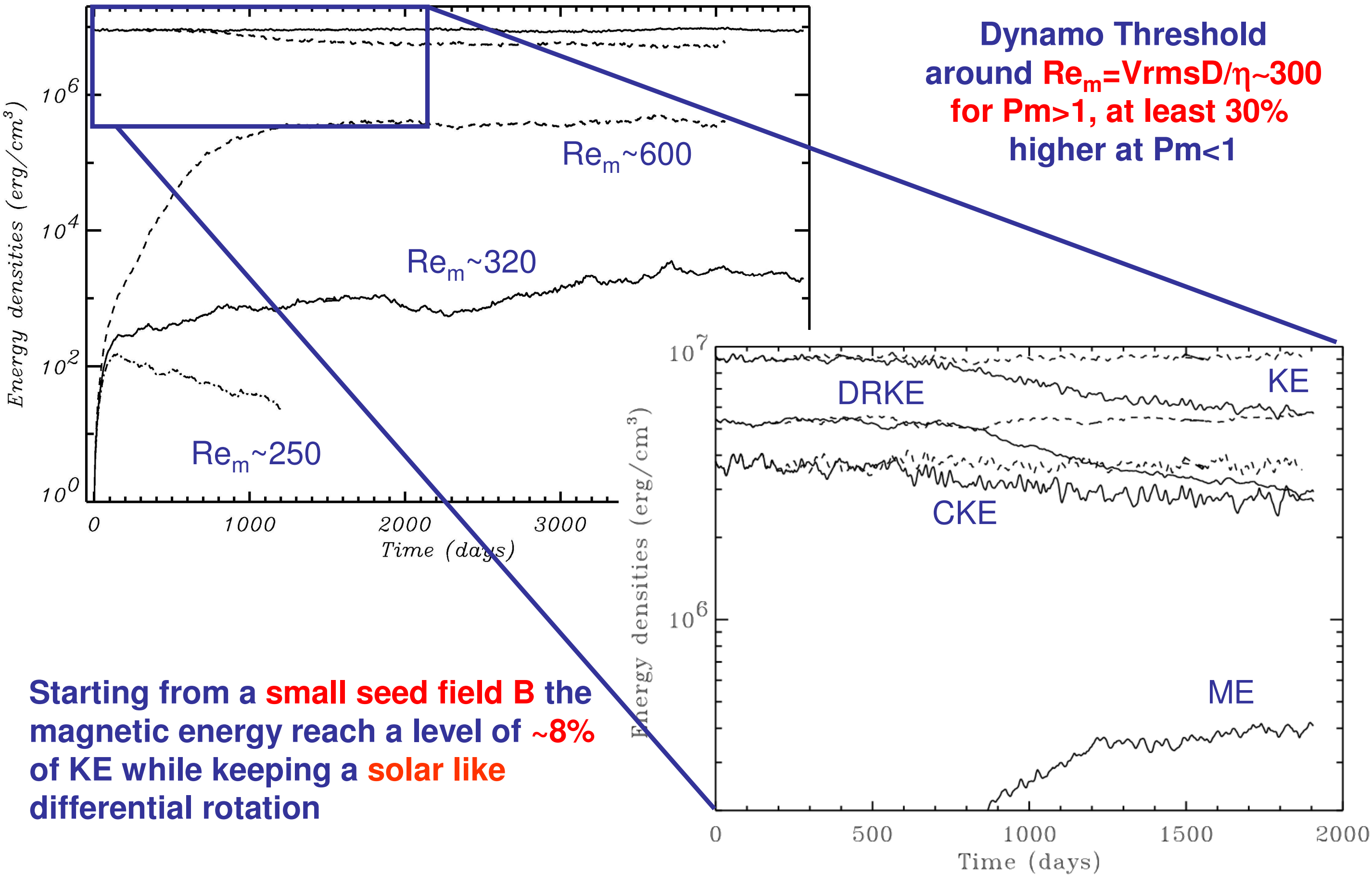

Dynamo Threshold around $Re_m = V_{rms} D/\eta \sim 300$ for Pm>1, at least 30% higher at Pm<1

Starting from a small seed field B the magnetic energy reach a level of ~8% of KE while keeping a solar like differential rotation

Magnetic Convection

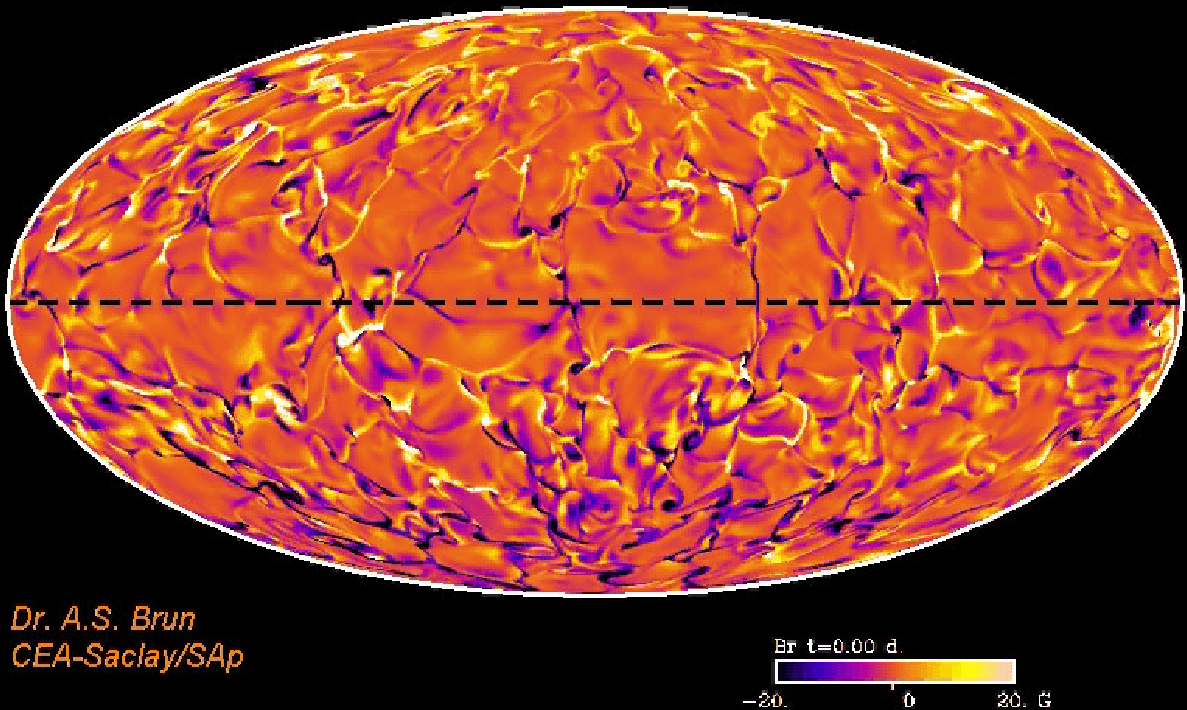

First High Res, low Pm (0.8) Dynamo of The Sun

Radial component of B

stretching and shearing of B (folding too)

Magnetic Convection

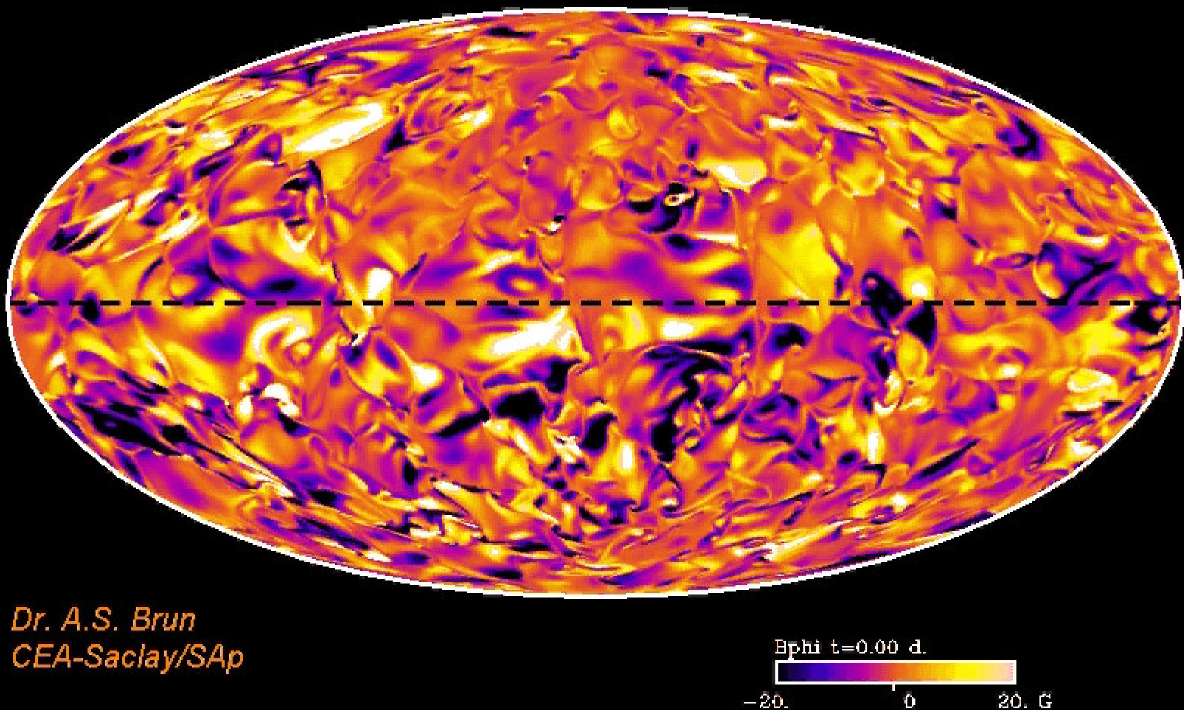

First High Res, low Pm (0.8) Dynamo of The Sun

Longitudinal component of B

stretching and shearing of B (folding too)

3-D Reconstruction of the inner and Coronal Field (potential approximation)

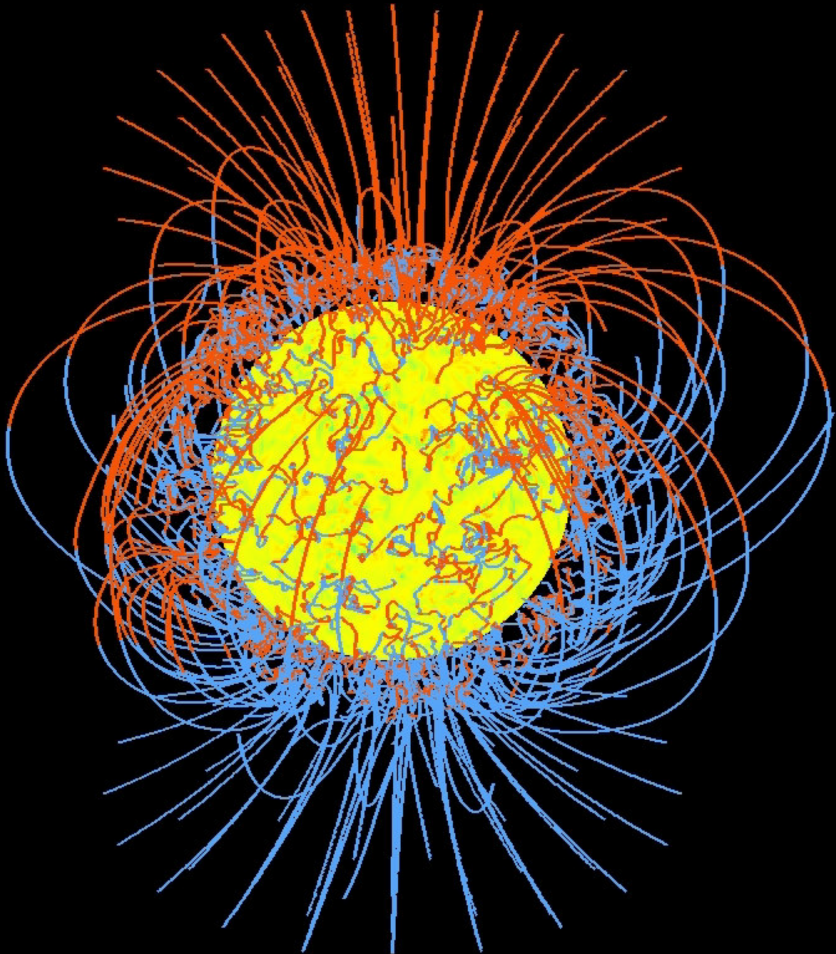

case G

(Brun et al., ApJ, 2004, Brun 2007)

Energy Decomposition vs r

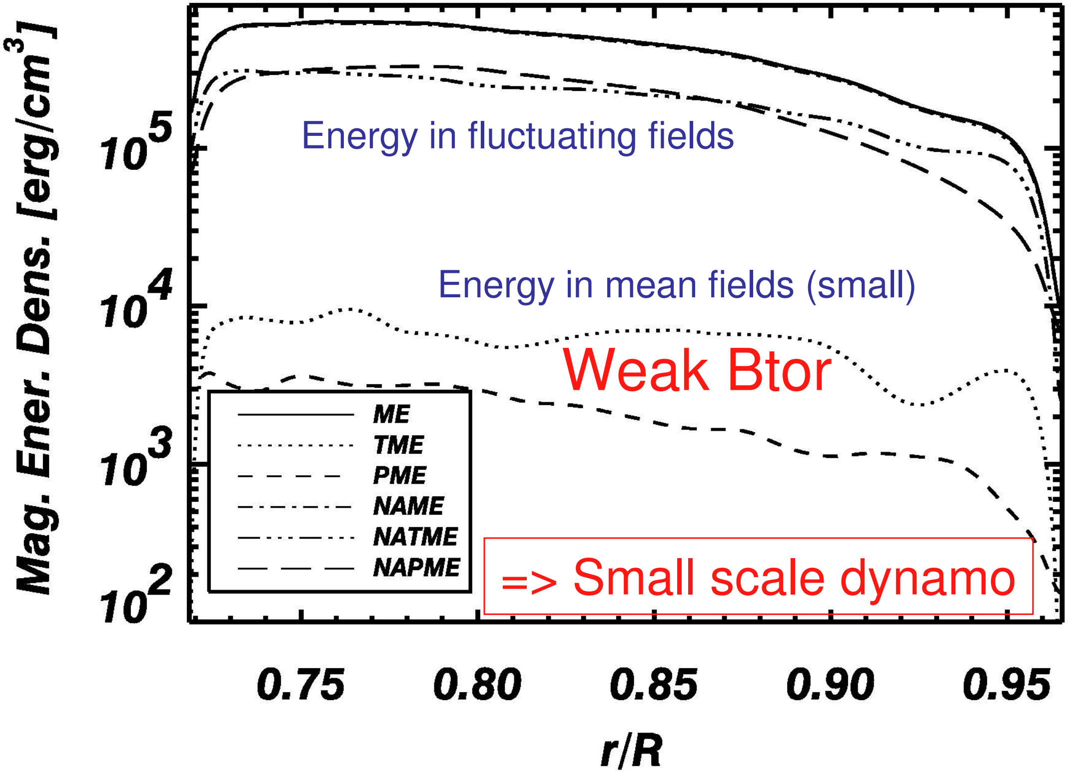

Magnetic energy peaks at the bottom of the shell, due to pumping by convective plumes

Mean Angular Velocity Ω

Ω quenching!

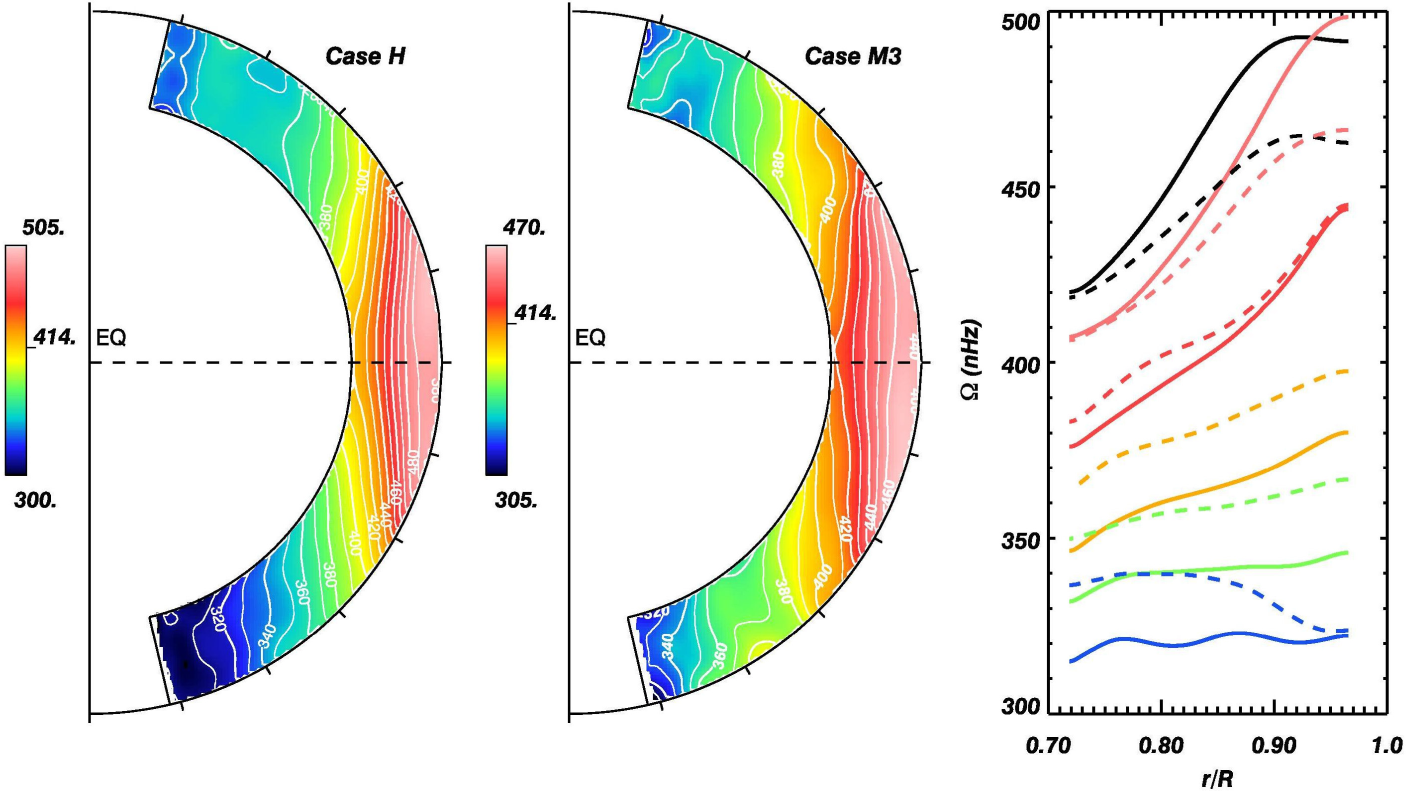

Initial state of differential rotation

Evolved state of differential rotation under the influence of the Lorentz force

Angular Momentum Balance in Presence of B

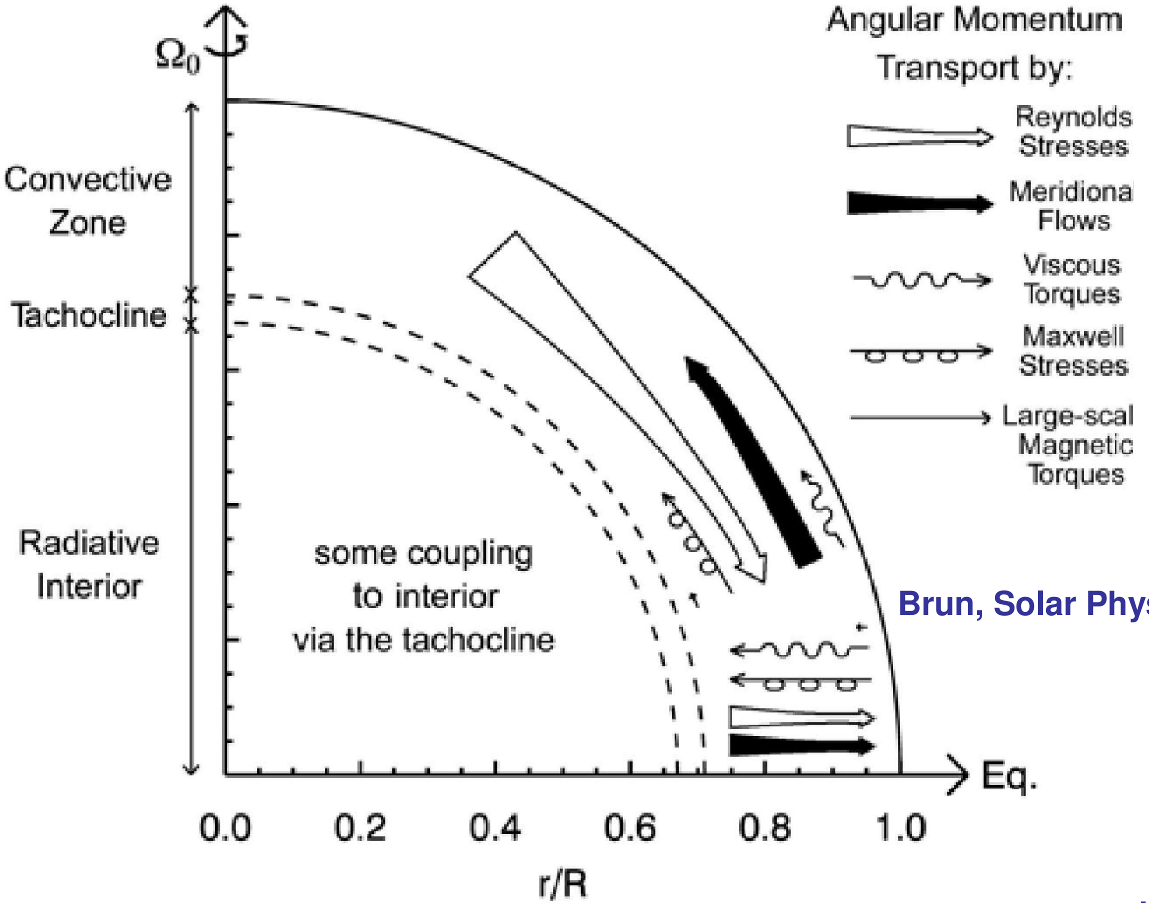

Brun, Solar Physics, 2004

The transport of angular momentum by the Reynolds stresses remains at the origin of the equatorial acceleration. The Maxwell stresses seeks to speed up the poles.

Influence of a Tachocline?

Browning et al. 2006, ApJL

See Juri's Talk

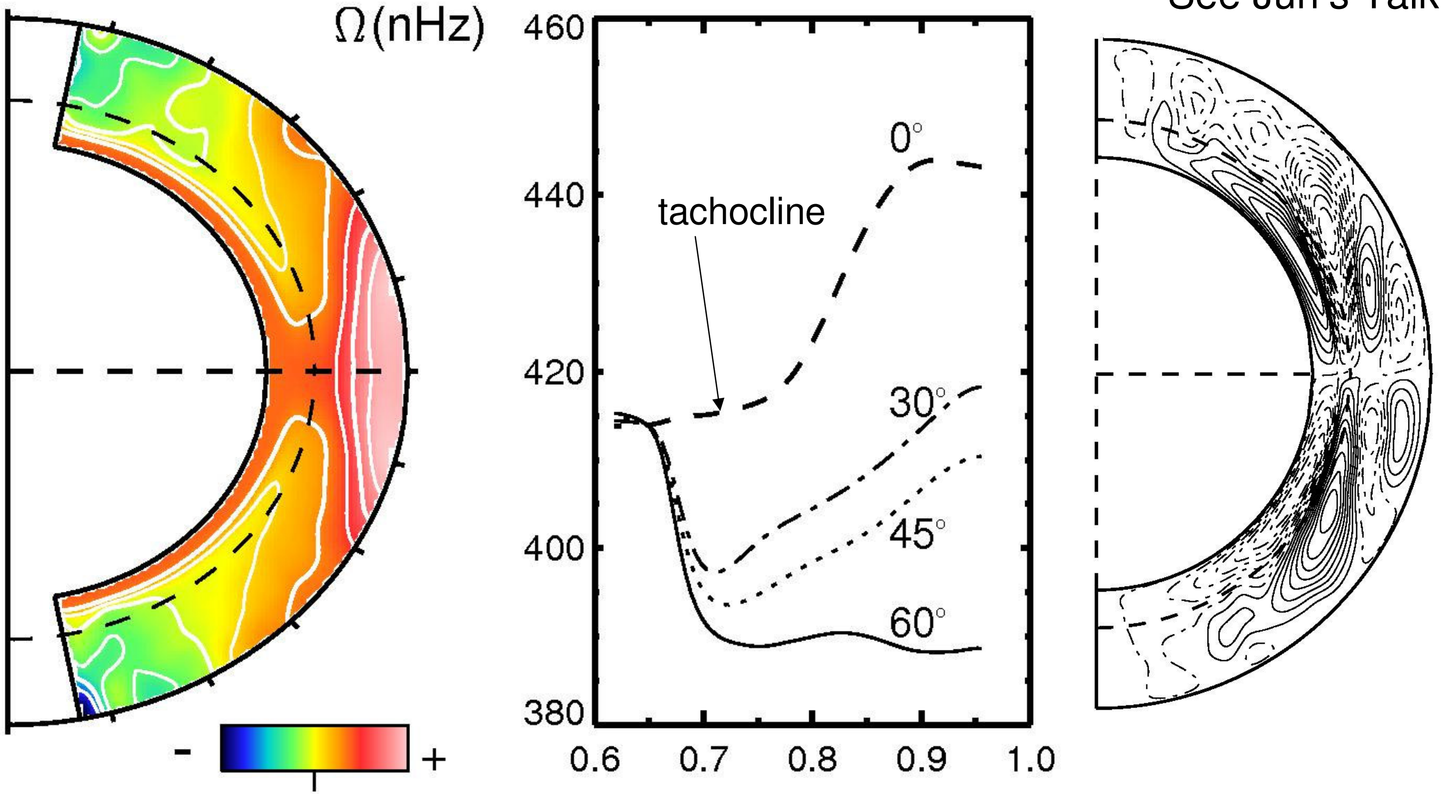

We impose a thermal wind in the stable lower zone compatible with a tachocline of shear maintained by a viscous drag.

3-D MHD Models of Solar Radiative Interior

Brun & Zahn 2006, A&A, 457, 665

Top of radiative zone (shear imposed by convection zone on top of RZ)

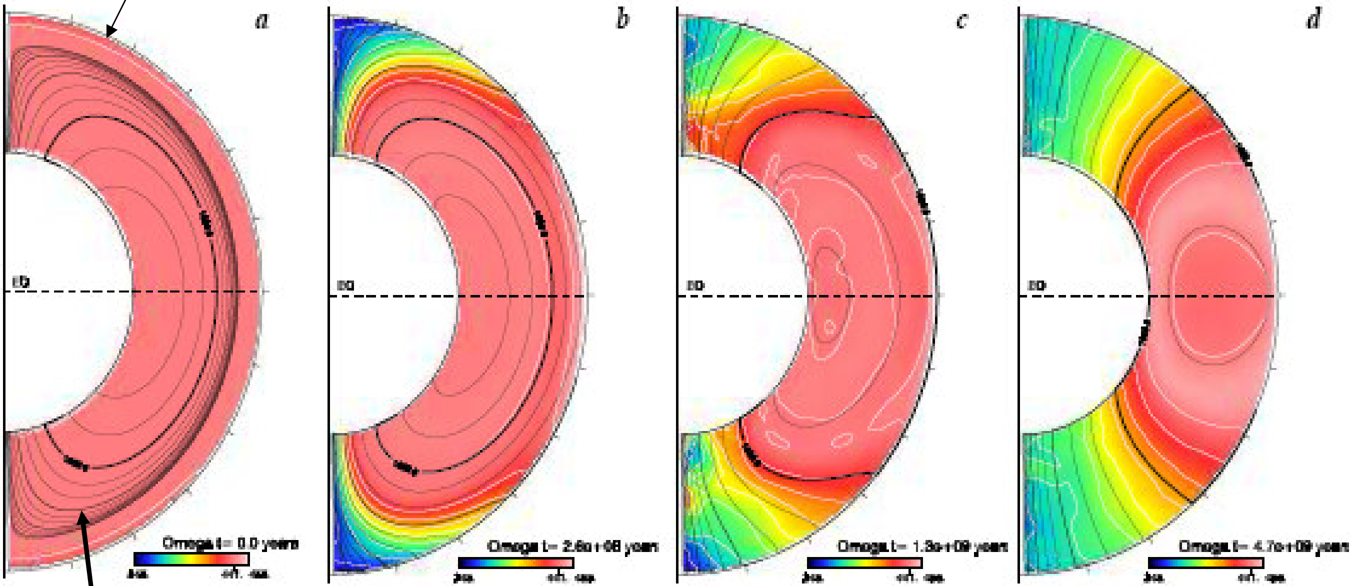

Fossil magnetic field

Final State: Ferraro's law of isorotation @ solar age

Interaction between a fossil field and the inward propagation of a latitudinal shear (e.g. the solar differential rotation)

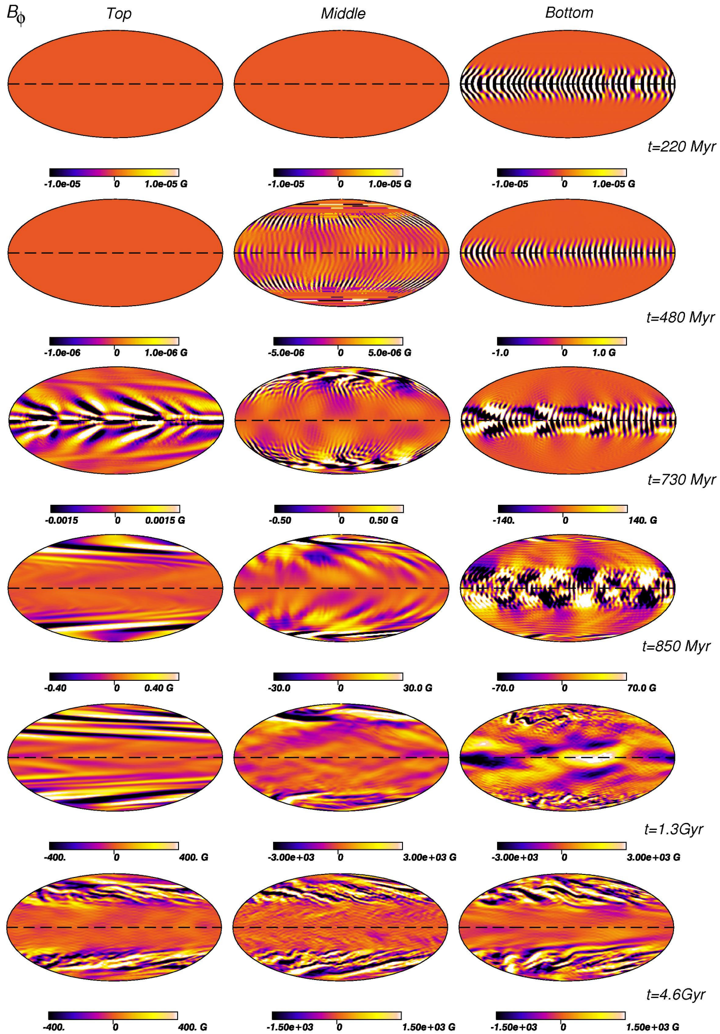

Hign m

Non-Axisymmetric Instabilities of Bpol and Btor

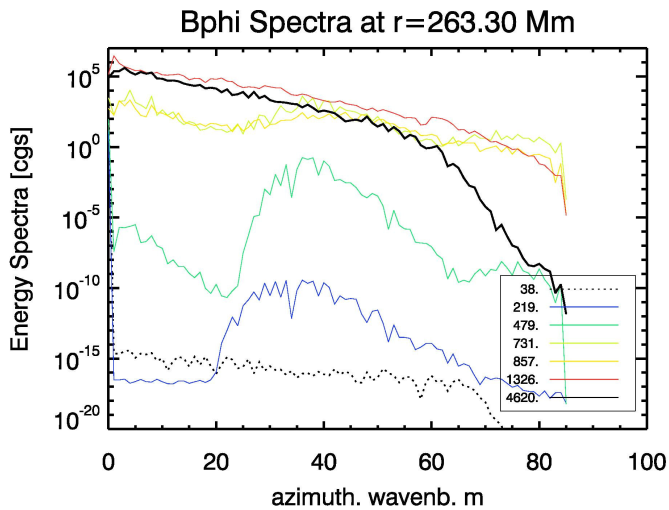

m=1

Dynamo In Radiative Interior?

(Spruit 2002, Braithwaite 2006, Zahn et al. 2007)

Brun & Zahn 2006, A&A

New Results on the Deep Sun

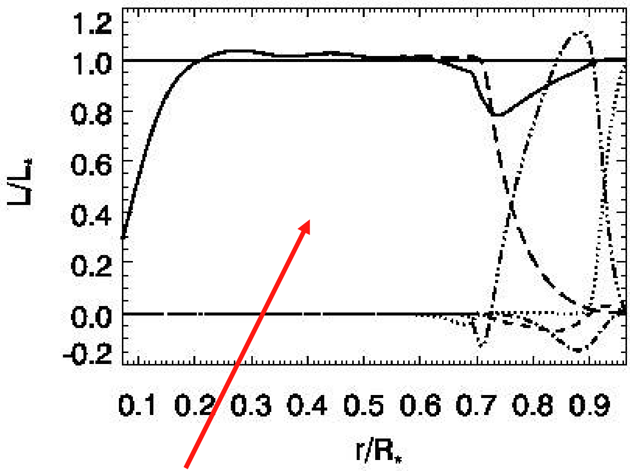

Extended RZ

Omega

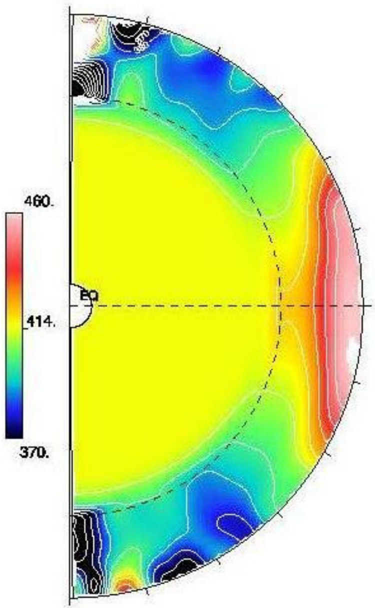

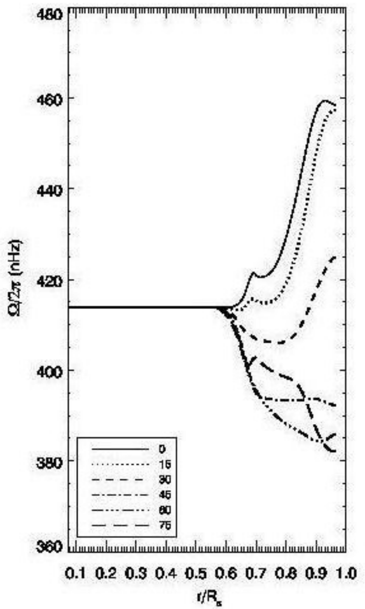

Equatorial Slices and Internal Waves

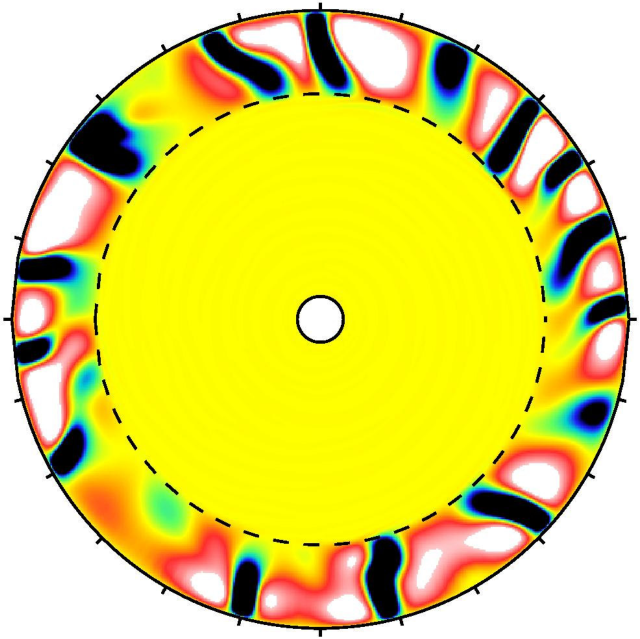

Vr

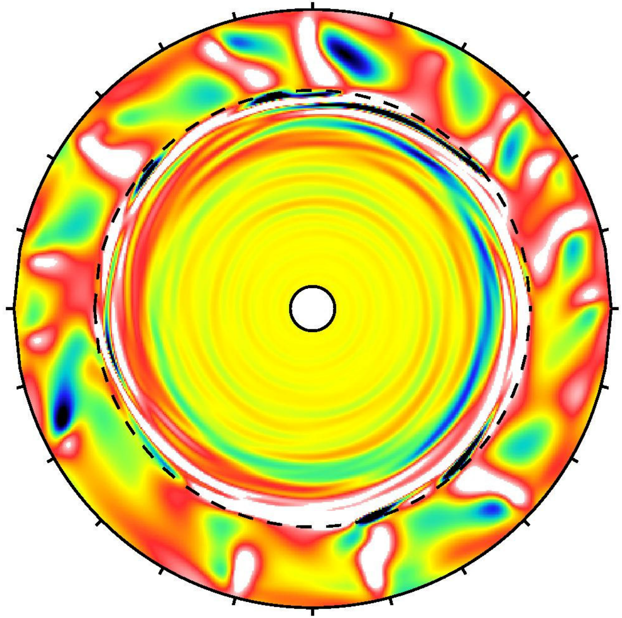

density

Equatorial Slices and Internal Waves

3-D view of Vr

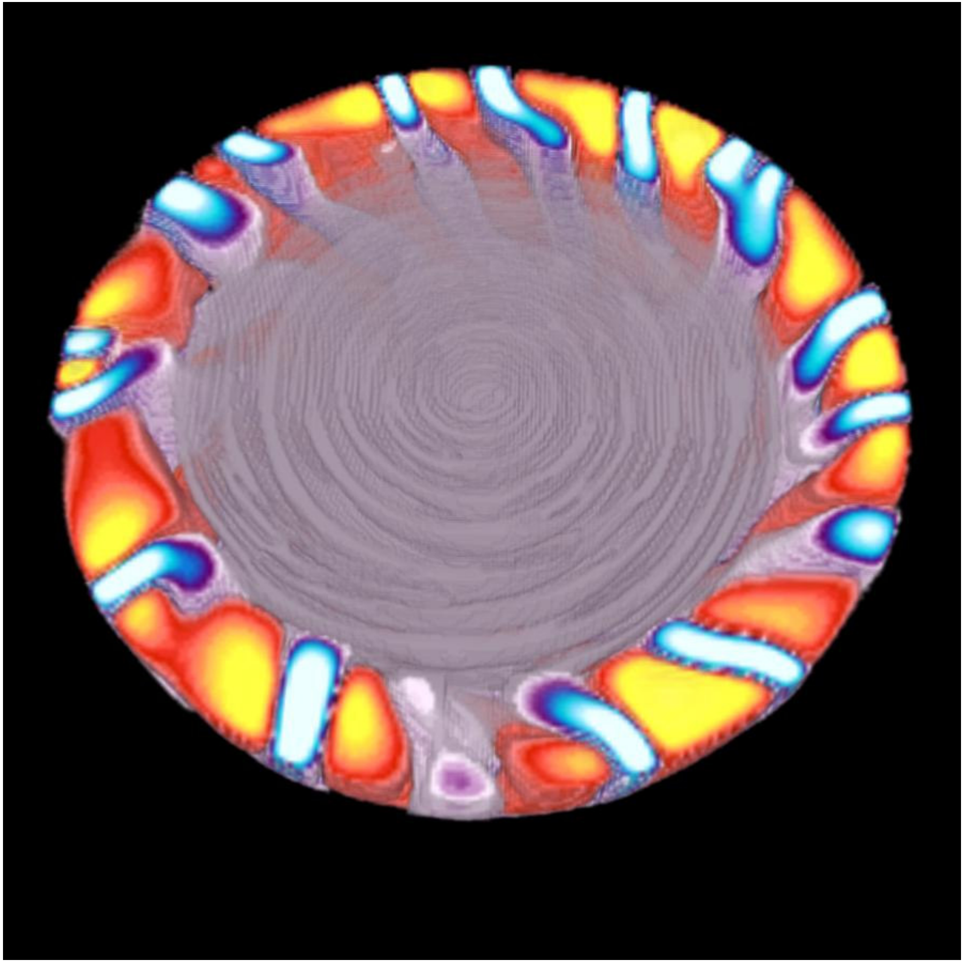

A Theoretical View of the Sun's Interior Dynamics

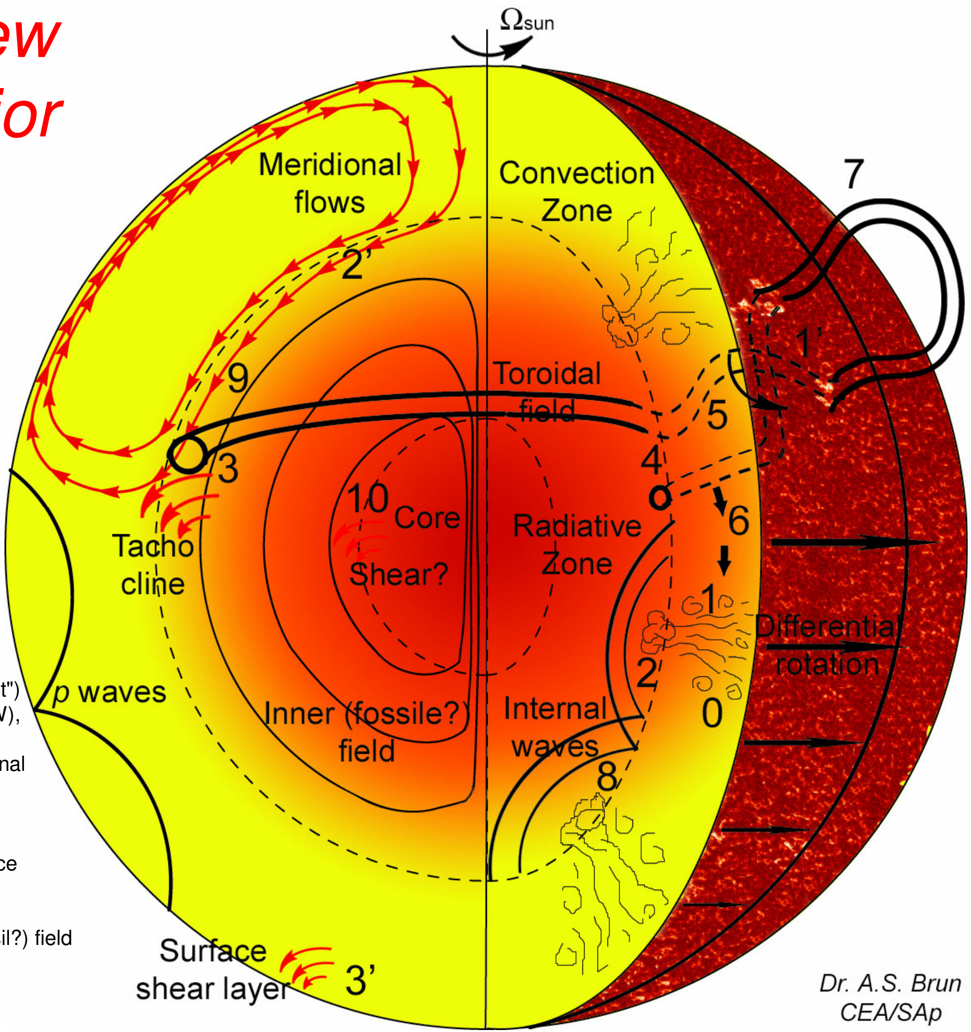

Figure Caption:
0: Turbulent convection (plumes)
1: Generation/self-induction of B field ("alpha-effect")
or 1': Tilt of active region, source of poloidal field
2: Turbulent pumping of B field in tachocline
or 2': Transport of B field by meridional flows
in CZ into the tachocline
3: Field ordering in toroidal structures by large scale
(radial and latitudinal) shear in tachocline ("omega-effect")
3': Surface shear layer, Solar sub surface weather (SSW),
surface dynamics of sun spot?
4: Toroidal field becomes unstable to m=1 or 2 longitudinal
instability (Parker's)
5: Rise (lift) + rotation (tilt) of twisted toroidal structures
6: Recycling of weak field in CZ
or 7: Emergence of bipolar structures at the Sun's surface
8: Internal waves propagating in RZ and possibly
extracting angular momentum
9: Interaction between dynamo induced field, inner (fossil?) field
in the tachocline (with shear, turbulence, waves, etc...)
10: Instability of inner field (stable configuration?)
+ shearing via "omega-effect" at nuclear core edge?
Is there a dynamo loop realized in RZ?

Dr. A.S. Brun
CEA/SAp

Convection Pattern and Diff Rot vs Omega for the Current Sun

Brown et al. 2007, AN and 2008 ApJ , Check Ben's poster

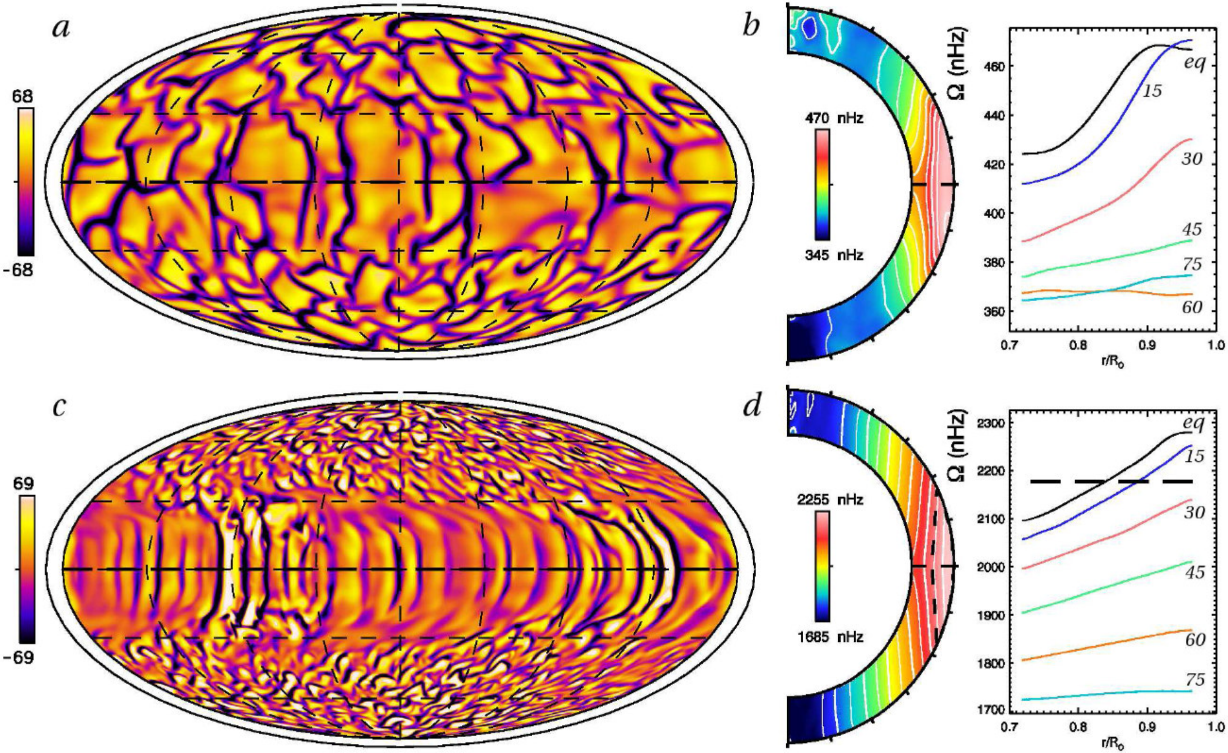

Fig. 1 Evolution of global-scale convective flows with increasing rotation rate for case G1 (a,b) and case G5 (c,d). Shown in (a, c) are global views, in Mollweide projection, of radial velocity near the stellar surface ($r = 0.95R_{\odot}$). Upflows are light while downflows are dark, with scales indicated in m/s. At high rotation rates a striking pattern of modulated convection emerges at low latitudes, consisting of spatially modulated or patchy convection. Shown in (b, d) are azimuthal averages of angular velocity Ω with radius and latitude. These have been further averaged in time over a period of roughly 200 days. Plotted at right are radial cuts of angular velocity at selected latitudes as indicated. The black dashed contour in (d) denotes the constant propagation rate of the nests in such modulated convection.

Scaling Law for Diff Rot Contrast and MC peak amplitude vs Omega0

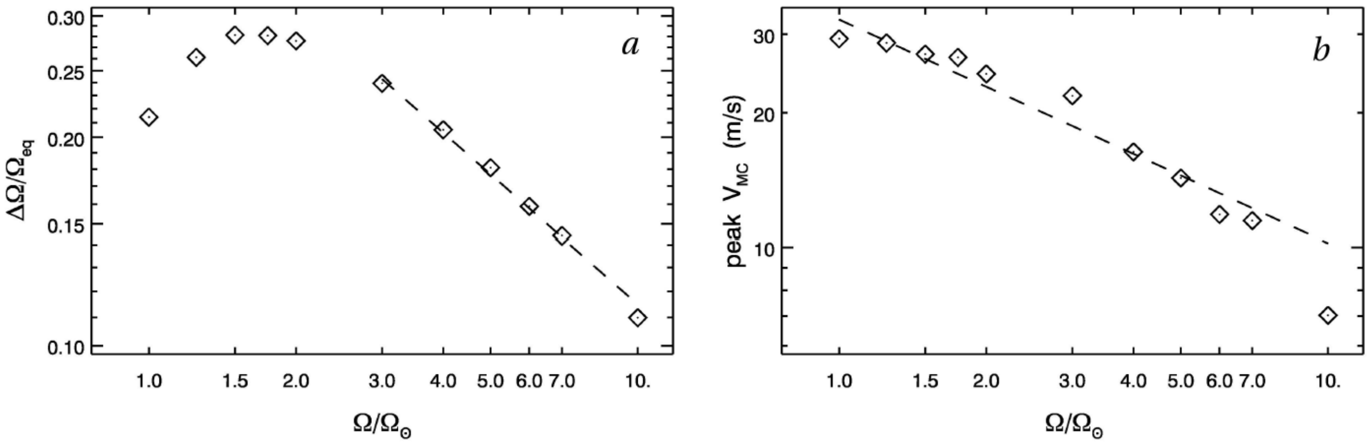

Fig. 2 Evolution of circulations with faster rotation: (a) angular velocity contrast $\Delta\Omega/\Omega_{\rm eq}$ plotted against bulk rotation rate $\Omega/\Omega_\odot$ of the simulations in logarithmic scaling. A power law with exponent $n = -0.6$ is overplotted. (b) Peak meridional circulations at the top of the simulation ($r = 0.96R_\odot$), showing a steep decline with more rapid rotation as the circulations break into multiple cells aligned with the rotation axis. Here a power law with exponent $n = -0.5$ overlies the data.

Faster rotation rate means weaker meridional flow!

Brown et al. 2007, AN
Brown et al. 2008, ApJ

With Magnetic fields, strong wreaths amidst the convection are found, see Juri's Talk and Ben Brown and Kyle Auguston Posters

MC flow in Young 10 Myr Suns

Ballot et al. 2007, ApJ

Faster rotation rate means weaker meridional flow!

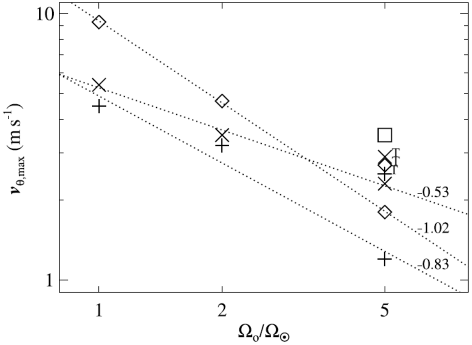

FIG. 12.—Surface velocity $\hat{v}_{\theta,\max}$ characterizing the meridional circulation intensity, plotted as a function of the rotation rate Ω_o. See caption of Fig. 10.

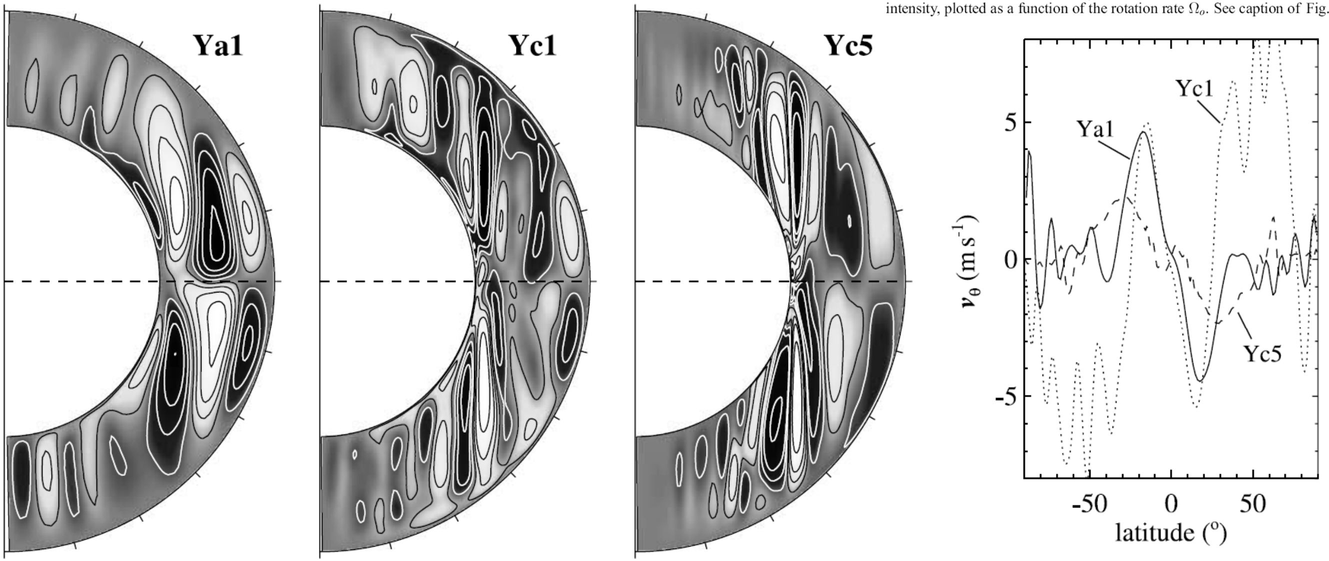

FIG. 11.—Meridional circulation in Ya1, Yc1, and Yc5. Maps show the mean mass flux circulation in the azimuthal plane. White lines over black background correspond to clockwise circulations, and black lines over white background to counterclockwise ones. The color scale is not linear to make visible even weak flows. Mean latitudinal velocity $\hat{v}_\theta$ profiles at the top of the shell are also plotted. Maps and profiles are obtained by averaging over longitude and time.

Core Convection in $2M_{sol}$ Star

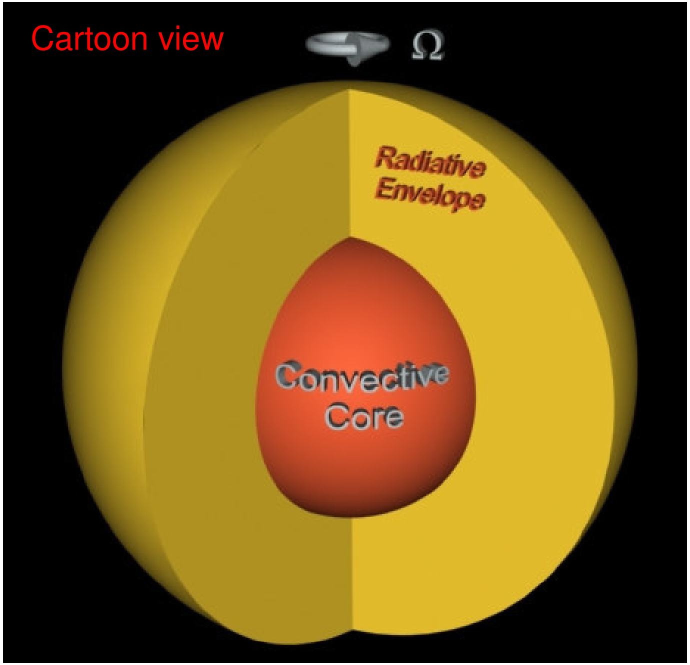

Star Caracteristic

$M=2M_{sol}$, $T_{eff}=8570$ K
$R=1.9\ R_{sol}$, $L=19\ L_{sol}$
$\Omega= 1, 4, 8$ or $1/10\ \Omega_{sol}$

EOS = Perfect gas law
Nuclear heat source ~ $\rho\varepsilon_0 T^8$
No gradient μ
Core omitted $r\sim0.02R$

Collaboration with M. Browning, N. Featherstone & J. Toomre

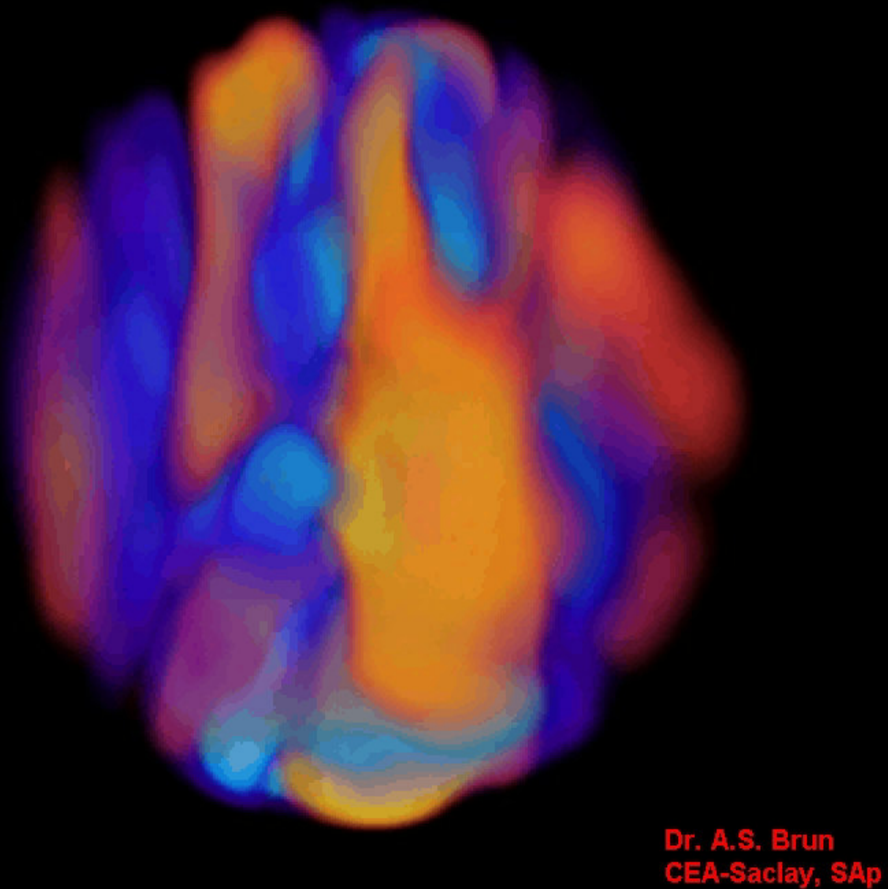

*Rendu 3D
de la
Vitesse radiale*

Re~140, P=0.25

(Browning, Brun & Toomre 2004, ApJ, 601, 512)

Dynamo effect (KE & ME interplay)

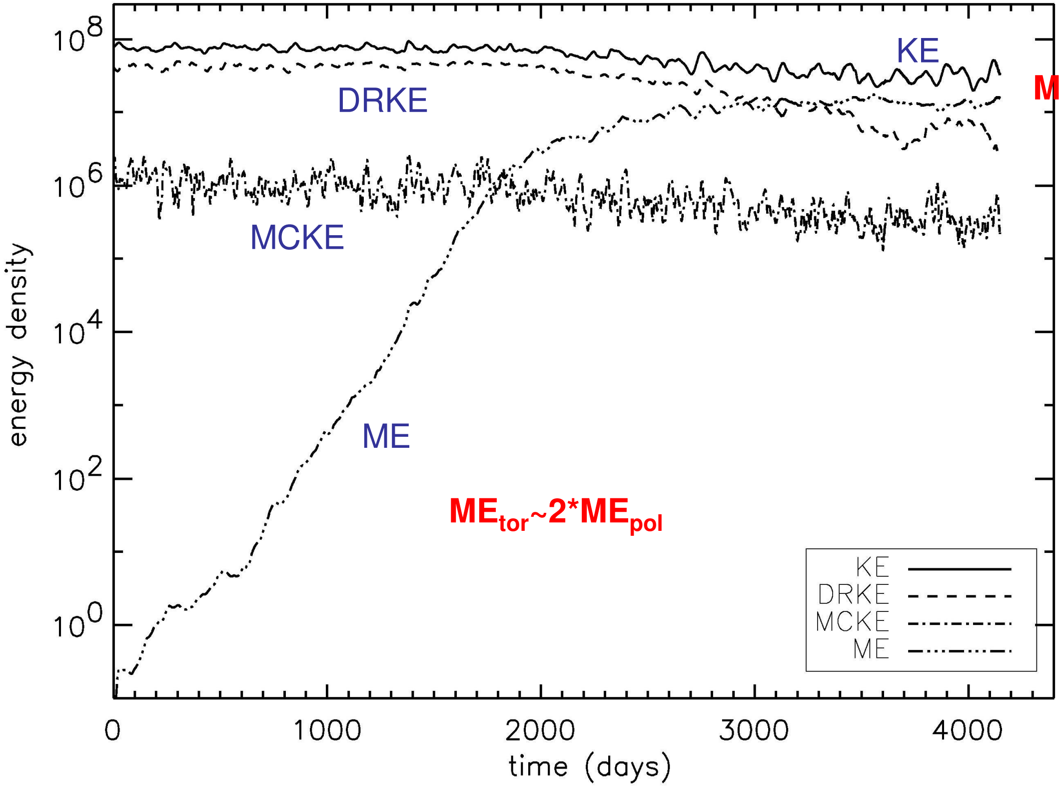

ME~40%KE

ME>DRKE & MCKE but < CKE

ME_{tor}~2*ME_{pol}

Lorentz force feedback jxB slow down Diff rot

(Brun, Browning, Toomre 2005, ApJ, 629, 461)

Core Dynamo

(Brun, Browning, Toomre 2005, ApJ, 629, 461)

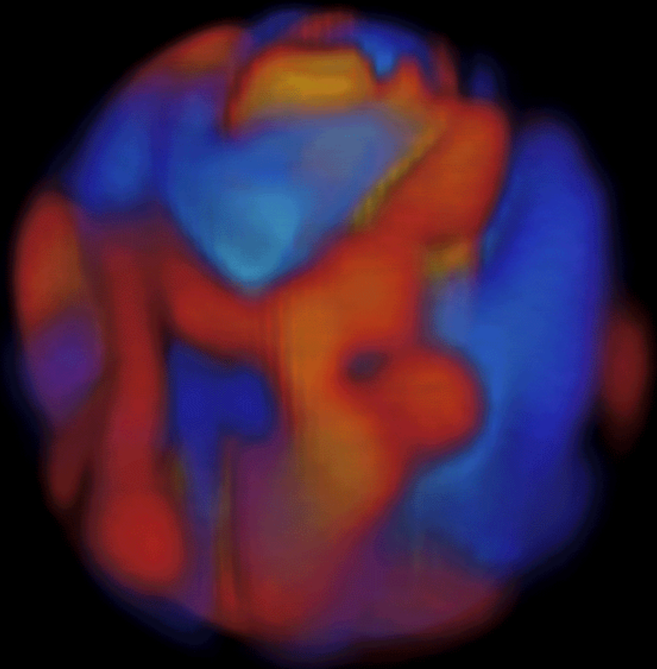

Vr

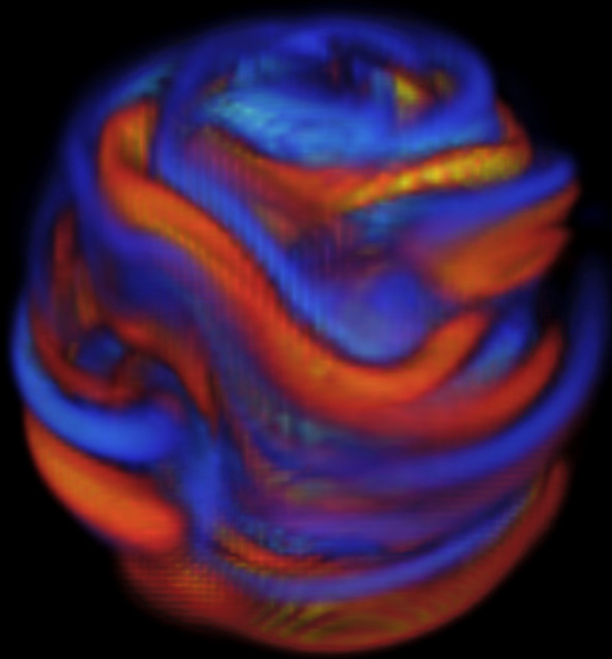

Bphi

Rotation Profile

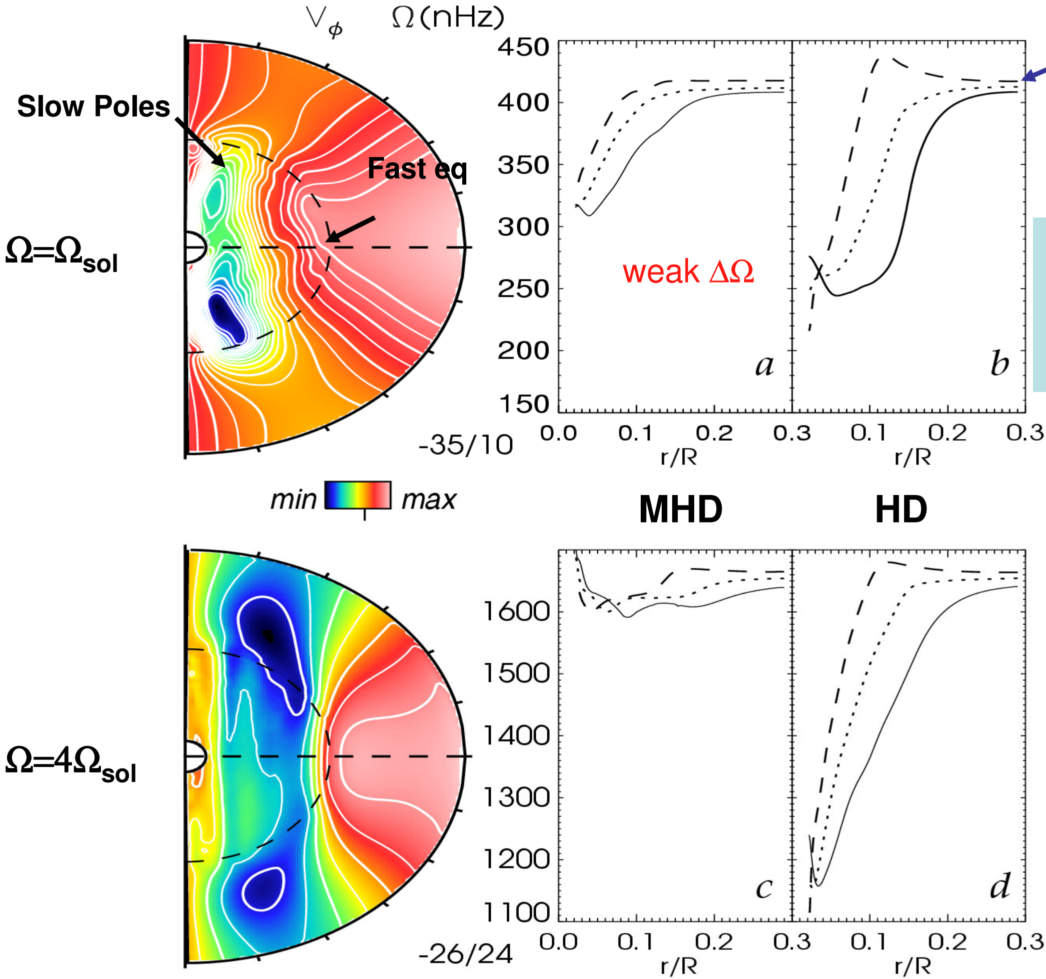

Almost rigid Rotation in RZ

Anngular momentum transport towards eq by RS opposed by MC and MX

Influence of fossile Field on core dynamo See N. Featherstone's Talk

Characteristics of the simulations with ASH

(Clune et al. 1999, Miesch et al. 2000, Brun et al. 2004, Palacios & Brun 2007)

Pop II RGB star @ the “*bump*” $M_* = 0.8 M_\odot$ $L_* = 425 L_\odot$ $R_* = 39 R_\odot$

computational domain

- $L \approx$ constant
- $\rho = [10^{-5}; 10^{-3}]$ g/cm^3
- $\Omega = \Omega_{sol}/10 = 2.6\ 10^{-7}$ rad s^{-1}
  or $\Omega_{sol}/50 = 5.2\ 10^{-8}$ rad s^{-1}

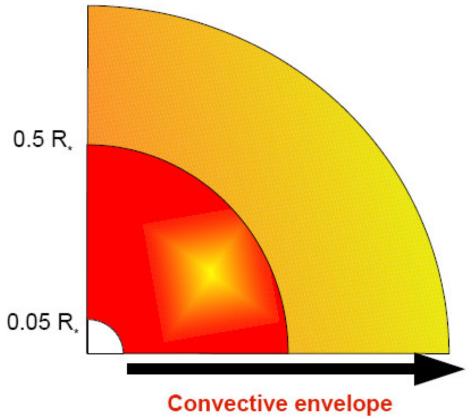

Rigid stress free boundaries

Prandtl number $\frac{\kappa}{\nu} = 1$

Energy Budget

Convective luminosity > L_* to compensate the negative kinetic luminosity

→ differs from MLT predictions

Negative kinetic energy represents up to 50% of the flux in the inner part of the domain

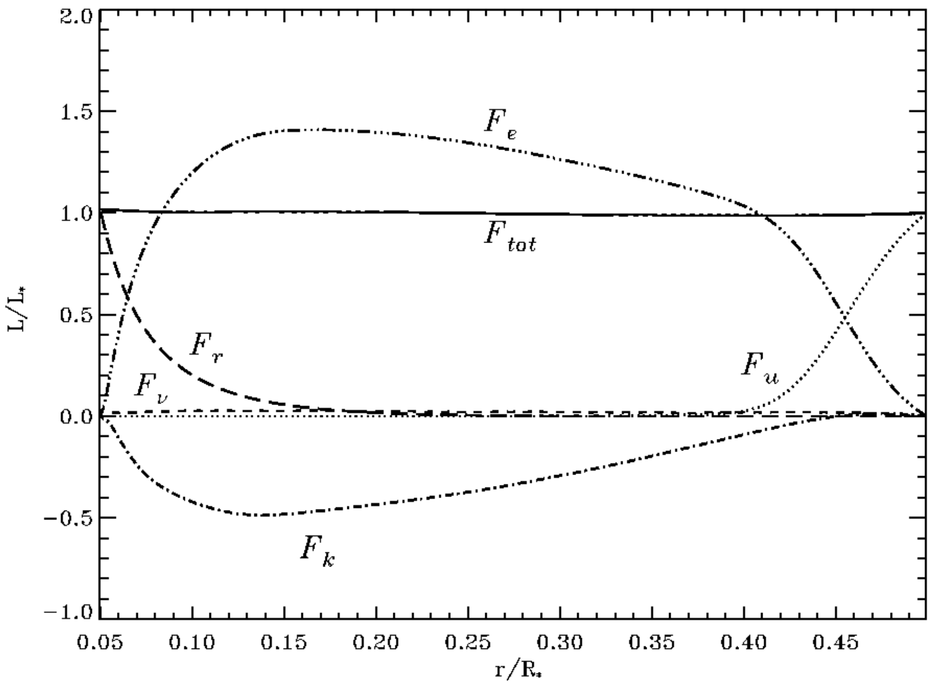

Convection

Omega= 1/10 solar

V_r @ domain top edge | T @ domain top edge | Enstrophy @ domain top edge

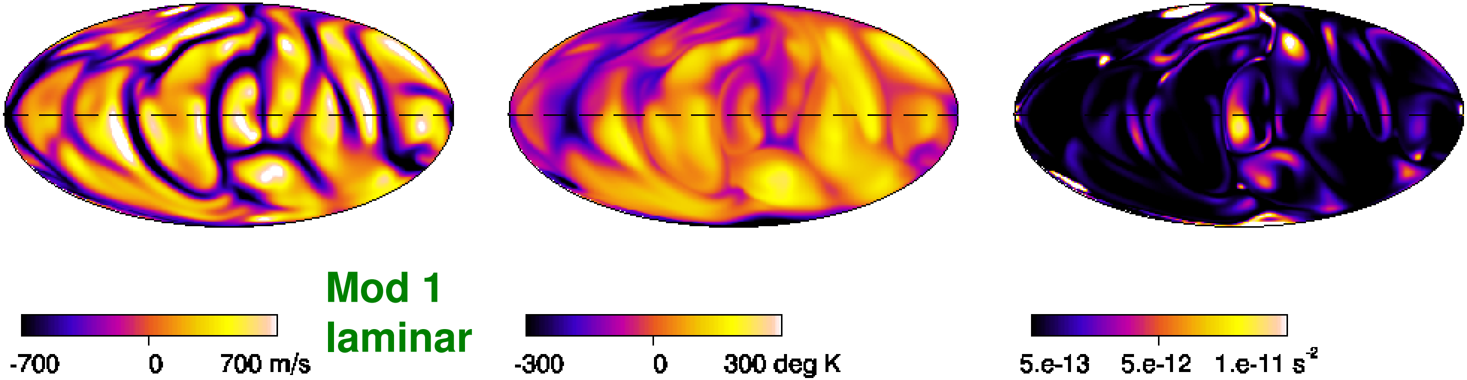

Mod 1 laminar

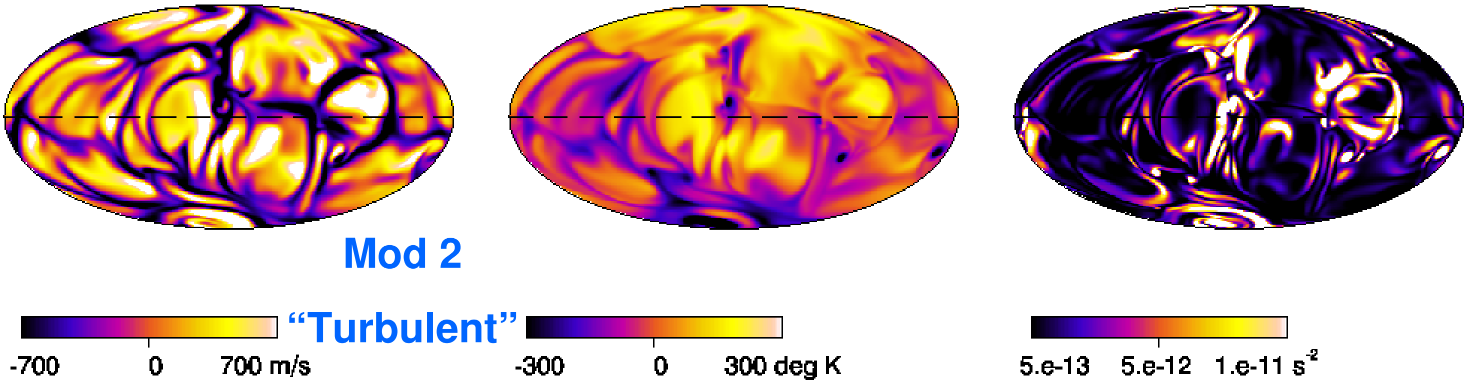

Mod 2 "Turbulent"

Rotation

Large differential rotation in the radial and latitudinal directions

Cylindrical rotation : only for “relatively” rapid rotators

Rotation law possesses strong radial dependancy, further 1/50 is shellular

1/10 solar

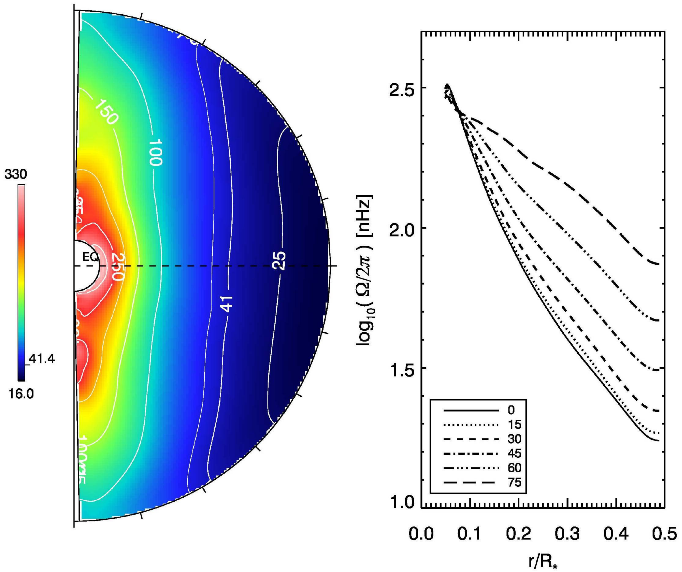

1/50 solar

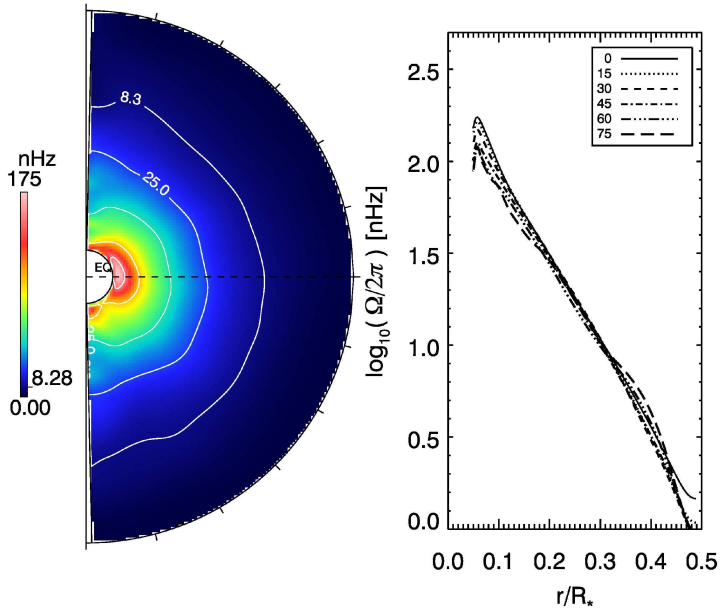

Palacios & Brun 2007, Brun & Palacios 2008

STARS^2 project: Understanding Stellar Dynamics and Magnetism

Asterosismology/Magnetism
SoHO/Corot/Espadon/XMM

3D MHD
High Performance
Simulations

(Brun et al. 2002, 2004, 2005, 2006, 2007, Ballot et al. 2007, Browning et al. 2004, Jouve & Brun 2007 a,b, Zahn, Brun & Mathis 2007, Brown et al. 2007)

Massive Stars

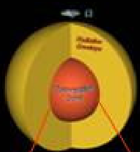

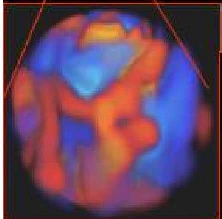

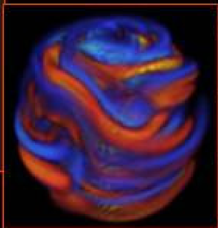

Sun

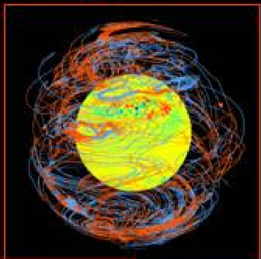

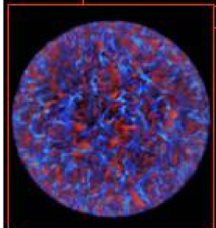

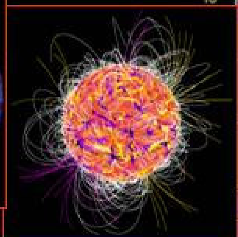

Evolved Stars (RGB)

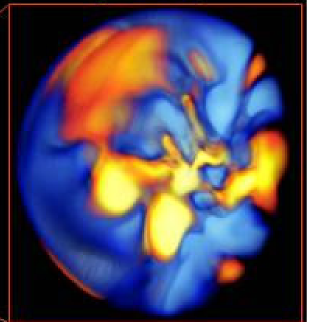

Young Suns

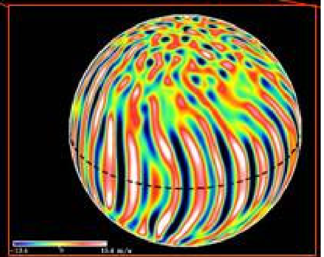

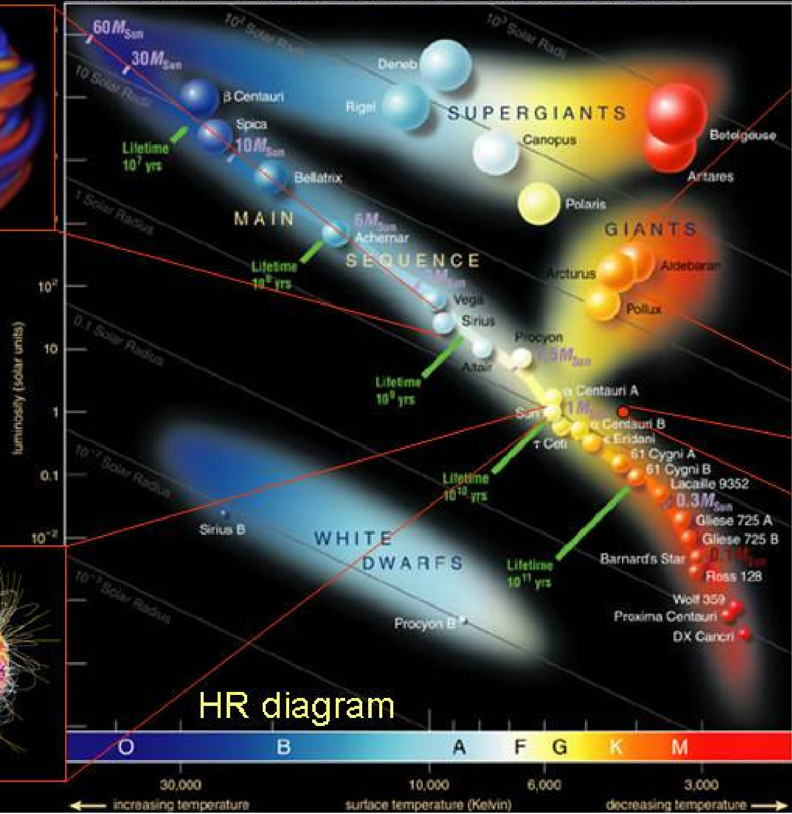

HR diagram